

# EFFICIENT HALLUCINATION DETECTION FOR LLMs USING UNCERTAINTY-AWARE ATTENTION HEADS

000  
001  
002  
003  
004  
005 **Anonymous authors**  
006 Paper under double-blind review  
007  
008  
009  
010

## ABSTRACT

011 Recent progress in large language models (LLMs) has led to systems capable of  
012 producing text with remarkable fluency. However, these models are still prone  
013 to factual inaccuracies, often referred to as “hallucinations”. One strategy to  
014 alleviate this issue is uncertainty quantification (UQ), but most existing approaches  
015 are computationally intensive or require supervision. In this work, we propose  
016 Recurrent Attention-based Uncertainty Quantification (RAUQ), an unsupervised  
017 and efficient framework for identifying hallucinations. The method leverages  
018 an observation about transformer attention behavior: when incorrect information  
019 is generated, certain “uncertainty-aware” attention heads, tend to reduce their  
020 focus on preceding tokens. RAUQ automatically detects these attention heads  
021 and combines their activation patterns with token-level confidence measures in a  
022 recurrent scheme, producing a sequence-level uncertainty estimate in just a single  
023 forward pass. Through experiments on twelve tasks spanning question answering,  
024 summarization, and translation across four different LLMs, we show that RAUQ  
025 consistently outperforms state-of-the-art UQ baselines. Importantly, it does so with  
026 minimal cost, less than 1% additional computation. Since it requires neither labeled  
027 data nor extensive parameter tuning, RAUQ serves as a lightweight, plug-and-play  
028 solution for real-time hallucination detection in white-box LLMs.  
029

## 1 INTRODUCTION

030 Large language models have become the de facto backbone of modern NLP systems; yet, the  
031 impressive fluency of their responses often conceals various inconsistencies known as “hallucinations”  
032 (Huang et al., 2025). There are several ways to address hallucinations, such as post-hoc  
033 verification using external knowledge bases (Min et al., 2023), incorporating retrieval-augmented  
034 generation to ground outputs in factual data (Lewis et al., 2020), or filtering/altering responses based  
035 on the uncertainty of a model (Kuhn et al., 2023; Farquhar et al., 2024). The latter approach, based  
036 on uncertainty, is the focus of this work.  
037

038 Uncertainty is a fundamental concept in machine learning, reflecting the fact that we usually lack  
039 complete information about the model’s predictions or parameters (Gal & Ghahramani, 2016; Houlsby  
040 et al., 2011; Hüllermeier & Waegeman, 2021). High predictive uncertainty typically signals a greater  
041 likelihood of hallucinations in the model output. Unlike verification methods that rely on external  
042 knowledge sources to detect hallucinations, uncertainty quantification (UQ) leverages the model’s  
043 internal capabilities, thereby mitigating issues related to the completeness of external sources and  
044 offering greater versatility. As shown in previous work, uncertainty scores can be used to detect  
045 hallucinations that arise due to limitations of LLM parametric knowledge or due to the ambiguity of  
046 requests in various generation tasks (Malinin & Gales, 2021; Geng et al., 2024; Baan et al., 2023),  
047 including question-answering, machine translation, text summarization, and speech recognition.

048 UQ for classification and regression tasks is a well-established area spanning decades of re-  
049 search (Zhang et al., 2019; He et al., 2020; Xin et al., 2021; Wang et al., 2022; Vazhentsev et al.,  
050 2023; He et al., 2024a). At the same time, UQ for generative tasks has only recently emerged as  
051 an active topic and still features open challenges. A crucial difference over classification is that  
052 an LLM performs not a single, but multiple conditionally dependent predictions. While recent  
053 work has proposed several promising techniques for quantifying predictive uncertainty in generation,  
e.g. (Kuhn et al., 2023; Farquhar et al., 2024; Duan et al., 2024; Qiu & Miikkulainen, 2024; Lin

et al., 2024b), prior methods have limitations. Namely, information-based scores such as maximum sequence probability (MSP) and token-level entropy are simple and fast, but often underperform on long-form generation tasks (Zhang et al., 2024; Vazhentsev et al., 2025a). Sampling-based scores offer stronger performance but incur large computational overhead (Kuhn et al., 2023; Lin et al., 2024b; Vashurin et al., 2025). Supervised confidence regressors (Azaria & Mitchell, 2023; CH-Wang et al., 2024), i.e., thin supplementary modules trained on supervised annotation, yield accurate scores, but require costly, task-specific annotation and often fail to generalize to out-of-distribution data or across tasks (Vazhentsev et al., 2025a). Thus, despite the recent surge of developments of UQ for LLMs, there is still a lack of an effective, versatile UQ method that (i) avoids the high computational costs associated with sampling-based approaches, and (ii) is robust across tasks and domains.

In this work, we aim to construct such a method. For this purpose, we peek into the attention weights of the transformer and identify patterns that are highly indicative of the presence of hallucinations. Self-attention matrices encode how strongly each newly generated token attends to its immediate context. We empirically observe a systematic drop in the attention weight to the preceding tokens in specific attention heads precisely at positions where the model later proves to be factually incorrect (Figure 1). Based on this finding, we argue that a small number of attention heads capture the behavior of transformer-based LLMs under uncertainty. We propose a method that automatically identifies such “uncertainty-aware” heads inside individual LLM layers and extracts the token-level signal from them. The method recurrently fuses this signal with token probabilities and confidence scores from previously generated tokens, capturing the conditional dependencies across generation steps. Finally, it aggregates token-level scores across the generated sequence and layers. The resulting sequence-level uncertainty score achieves state-of-the-art performance and demonstrates high robustness to the choice of its single hyperparameter. Moreover, since attention weights are readily available at inference time for white-box LLMs, the method requires no additional generation passes and adds almost no computational overhead to response latency.

### Contributions:

1. **In-depth analysis** of attention-based patterns in LLMs associated with hallucinations, which uncovers what we term “uncertainty-aware” heads, i.e., attention heads whose signals notably correlate with hallucination occurrences.
2. **RAUQ (Recurrent Attention-based Uncertainty Quantification)** – an *unsupervised* UQ method that turns raw attentions and LLM probabilities into reliable uncertainty scores while adding only <1% latency. RAUQ requires *no* task-specific labels or tuning of hyperparameters for a particular LLM, making it an easy plug-and-play for white-box LLMs.
3. **Thorough experimental evaluation** on four LLMs and 12 benchmarks, spanning summarization, translation, and question answering, showing that RAUQ achieves state-of-the-art results over 15 baselines. We also demonstrate the importance of each component within the method and illustrate that each individually could improve other UQ methods.

## 2 RELATED WORK

Several recent studies have proposed attention-based UQ methods for detecting hallucinations in LLM-generated outputs.

Zhang et al. (2023) use attention weights to propagate uncertainty across generation steps by capturing conditional dependencies, helping to mitigate overconfidence from prior hallucinations. However, attention plays a secondary role, with the method mainly relying on probability and entropy.

Yuksekgonul et al. (2024) perform a mechanistic investigation of attention patterns linked to LLM factual errors and propose a supervised UQ method called SAT Probe. They associate hallucinations with weak attention to so-called “constrained” tokens in the prompt – key prompt elements that narrow down the scope of the answer. However, their experiments show that SAT Probe performs only on par with or slightly better than baselines. In a similar vein, Contextualized Sequence Likelihood (Lin et al., 2024a) leverages attention to important tokens in the input context to reweight the contribution of token logits when computing weighted sequence likelihood. Lookback Lens (Chuang et al., 2024) leverages attention maps to construct features for a supervised hallucination detector. The authors hypothesize that hallucinations correlate with less attention paid to the input context. They compute

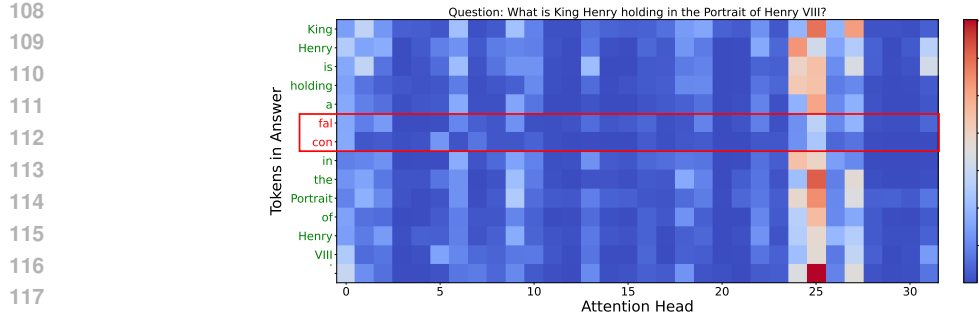


Figure 1: Attention weights in the 29th layer of Llama 3.1 8B from each generated token to its preceding token, given the prompt *What is King Henry holding in the Portrait of Henry VII?*. The  $y$  axis specifies the generated tokens, and the  $x$  axis specifies the attention heads. Warmer colors indicate higher attention values. The output contains the factually incorrect token *falcon* (the correct answer is *gloves* and *dagger*). Notably, the 25th attention head stands out by consistently assigning relatively high attention to the preceding token. However, for the hallucinated token *falcon*, this attention drops sharply – potentially serving as a signal for hallucination detection.

the ratio between cumulative attention weights to tokens in the answer and the prompt and train a linear classifier on top of these features. Attention-based features are also used in Trainable Attention-Based Dependency (Vazhentsev et al., 2025a). This method adds recurrence when computing uncertainty for subsequent tokens. It demonstrates strong results for in-domain tasks, outperforming Lookback Lens, but both methods lack generalization due to their supervised nature.

Finally, Sriramanan et al. (2024) recently proposed the Attention Score method, where they compute a length-normalized sum of log attention weights to preceding tokens across the prompt and the answer. Lower scores signal the presence of hallucination.

Although recent studies show that attention weights offer valuable signals for detecting hallucinations in LLM outputs, existing methods suffer from various limitations that hinder their effectiveness. SAT Probe, Lookback Lens, and TAD are supervised and show limited generalization beyond their training domain. Zhang et al. (2023) and Lin et al. (2024a) leverage attention only as a supplement to other scores. Sriramanan et al. (2024) do not select proper attention heads before averaging, and allow the attention weights from prompt tokens to participate in the aggregation for the final score, which causes underperformance.

In this work, we aim to overcome the limitations of existing methods. To this end, we identify strong and generalizable attention-based patterns for LLM hallucination detection, isolate the key techniques required to effectively exploit these patterns, and develop a robust *unsupervised* UQ method that achieves state-of-the-art performance.

### 3 HALLUCINATION-ASSOCIATED PATTERNS IN ATTENTION MAPS

We analyze the model’s attention maps when an LLM generates correct vs. incorrect outputs. We start with an analysis of attention weights to the immediately preceding token, i.e.  $a_{i,i-1}^{lh}$  – attention weight to the  $\{i-1\}$ -th token during the generation of  $i$ -th token from the layer  $l$  and attention head  $h$ . Let  $N$  be the number of generated tokens in the answer,  $H$  the number of attention heads in each layer, and  $L$  be the number of layers in the LLM. For illustration, we use the Llama 3.1 8B model.

**Difference between attention weights for hallucinated and non-hallucinated tokens.** Figure 1 presents an example of the attention weights to preceding tokens  $a_{i,i-1}^{lh}$  in one of the LLM layers for the input question from the TruthfulQA dataset: *What is King Henry holding in the Portrait of Henry VII?* Most of the generated tokens are aligned with the question. However, the token *falcon* represents a hallucination, i.e. it is factually incorrect (the answer should be *glove and dagger*).

For most attention heads, the weights to previous tokens remain low across all generated tokens. In contrast, the 25th head exhibits a distinct pattern: it assigns relatively high attention to the

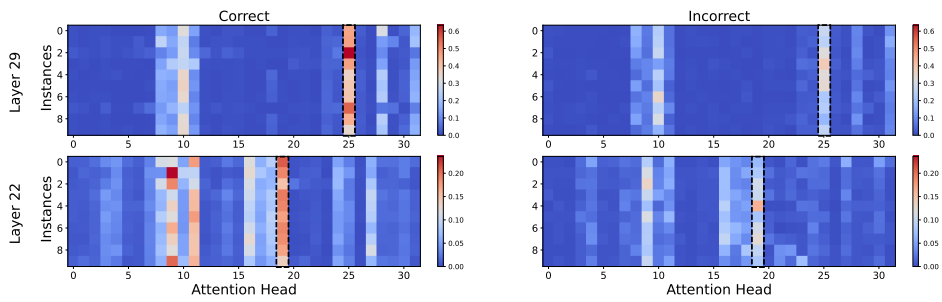


Figure 2: Average attention weights to the preceding token, aggregated over all answer tokens for questions from the TruthfulQA dataset using Llama 3.1 8B. The top 10 highest- and lowest-quality answers, as determined by a quality metric, are labeled as correct and incorrect, respectively. The black dashed box highlights the head with the highest average attention.

preceding token for non-hallucinated (i.e., correct) tokens, but this attention drops significantly for the hallucinated token *falcon*.

This example demonstrates that attention weights from a small subset of attention heads can notably correlate with the factual correctness of generated tokens. While the choice of layer and head might vary, this case suggests that certain heads in specific layers are “uncertainty-aware”, i.e., they are sensitive to generation accuracy and could help to identify hallucinations. More examples of the similar pattern for Llama and other LLMs are presented in Figures 6 to 9 in Appendix F.

**Difference between average attention weights for incorrect and correct answers.** We begin by selecting 10 correct and 10 incorrect answers generated by the LLM. To evaluate the correctness of each answer, we use AlignScore – a continuous metric that quantifies semantic similarity between the generated response and the gold-standard answer (Zha et al., 2023). We sort all generations by their AlignScore, and designate the top 10 as correct answers and the bottom 10 as incorrect.

Then, we compute the average attention weight to the previous token across all tokens in the answer using the attention heads in the 29th and 22nd layers of the LLM, i.e.  $\bar{a}^{lh} = \frac{1}{N-1} \sum_{i=2}^N a_{i,i-1}^{lh}$ . Figure 2 presents the resulting values, where each row corresponds to a single selected answer, and each column indicates the average attention weight from a specific head.

The attention maps in the figure demonstrate that certain heads consistently assign higher average attention when the LLM generates correct answers as compared to incorrect ones. Moreover, there is a notable correlation between the quality of the answer and average attention (see Figure 3b). This way, we empirically discovered a pattern for assessing the correctness of LLM generations. From a theoretical perspective, eigenvalue analysis of attention weights reveals similar hallucination patterns, justifying the focus on weights to the previous token, as these are correspond to the log-determinant of the attention matrix (Sriramana et al., 2024).

**Should we select uncertainty-aware heads, and how should we do it?** We compute the average attention score  $\bar{a}^{lh}$  across tokens in two scenarios: (1) attention values are averaged across all heads in a layer, i.e.  $\bar{a}^l = \sum_{h=1}^H \bar{a}^{lh}$ ; (2) attention values are extracted from a single head with the *highest* average attention across tokens, i.e.  $\bar{a}^{lh_l}$ , where  $h_l = \arg \max_{h=1 \dots H} \bar{a}^{lh}$ . Figure 3a compares the resulting values for correct and incorrect answers.

When using only the selected attention head, we observe a clear difference in the values between correct and incorrect answers. However, averaging attention across all heads eliminates this difference. This once again highlights the importance of focusing on specific uncertainty-aware heads. These heads can be identified by selecting those with the highest average attention weights across all tokens.

**Do we need to look further back at preceding tokens to better detect hallucinations?** We analyze the attention weights to multiple preceding tokens. Here, we compute  $a_{i,i-k}^{lh}$  – an attention weight to the  $\{i-k\}$ -th token ( $k$ -th preceding token),  $k = 1, \dots, 6$ . Figure 4 shows the difference between the average attention weights of the correct and incorrect answers.

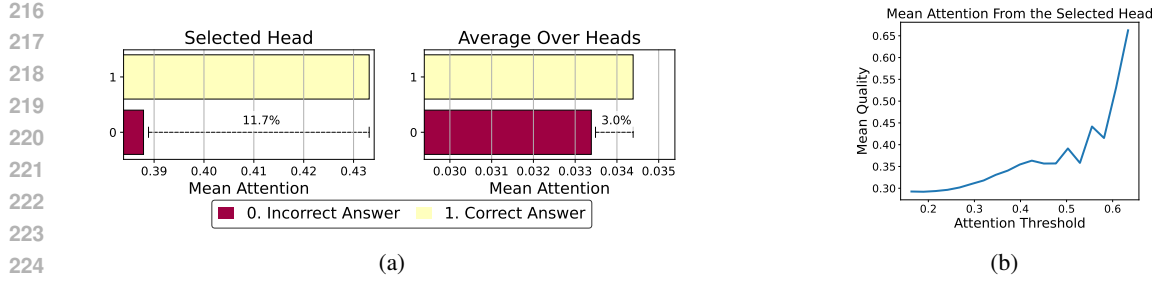


Figure 3: Attention weights to the preceding token averaged across all tokens in the generated responses of Llama 3.1 8B on TruthfulQA. a): Comparison between incorrect ( $\text{AlignScore} < 0.1$ ) and correct ( $\text{AlignScore} > 0.9$ ) answers. Attention values are presented for two scenarios: (left) from the selected head with the highest average attention; (right) averaged across all heads. b): The relationship between average response quality and the average attention weight in the selected head.

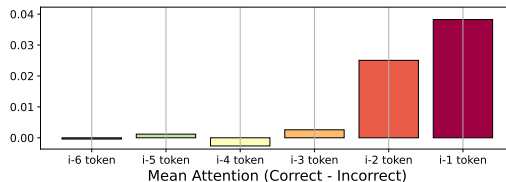


Figure 4: Difference between correct ( $\text{AlignScore} > 0.9$ ) and incorrect answers ( $\text{AlignScore} < 0.1$ ) in average attention weights to preceding tokens during the generation of answers for the questions from the TruthfulQA dataset using Llama 3.1 8B.

We see that the attention weights differ substantially between correct and incorrect answers only for the two preceding tokens, with almost zero differences observed for earlier tokens. Notably, the difference is substantially larger for the first preceding token as compared to the second one.

**Summary.** Our analysis uncovers attention patterns associated with the factuality of individual tokens and LLM responses in general. A key observation is that such systematic patterns emerge only for a small subset of specific attention heads. Effectively leveraging them requires first identifying the relevant uncertainty-aware attention heads. We also observe that the immediately preceding token provides the strongest signal, leading us to focus solely on it in our method design and subsequent experiments. Below, we leverage the insights from this mechanistic investigation to develop a new *unsupervised* UQ method for LLMs.

## 4 RAUQ: RECURRENT ATTENTION-BASED UNCERTAINTY QUANTIFICATION METHOD

**Key ideas and theoretical grounding.** RAUQ, to be effective, integrates three key ideas.

The first idea is that *attention weights to previous tokens contain patterns indicative for hallucination detection*. This is grounded in previous works on attention-based UQ. Sriramanan et al. (2024) illustrate that attention weights contain patterns indicative of hallucinations through eigen-analysis of attention kernels. They use only the attention weights to the previous token, as these correspond to the eigenvalues of the lower triangular attention matrix, and their sum exactly equals its log determinant. We reveal a similar pattern through a mechanistic analysis of attention weights, examining the correlation between hallucinations and attention weight distributions, as shown in Section 3.

In the second idea, we follow (Zhang et al., 2023; Vazhentsev et al., 2025a) and acknowledge that computing uncertainty at the generation step  $i$  requires propagating uncertainty from previous steps due to the conditional dependencies in the probability distribution modeled by the LLM. Namely, even if previous tokens were generated with high uncertainty, a model may condition on them and be highly confident in its current token prediction. To take this issue into account, we introduce a formulation that *recurrently propagates uncertainty from previous steps*.

270 The third idea is *attention head selection*. We observe that the majority of heads are not indicative of  
 271 hallucinations (Figure 3a). Therefore, we suggest selecting the most contrastive head that has the best  
 272 potential for discriminating between hallucinations and non-hallucinations. Our findings are well  
 273 supported by prior mechanistic interpretability studies of attention heads, which have shown that  
 274 different heads serve distinct functions Elhelo & Geva (2025).

275 Let  $\mathbf{x}$  be the input sequence and  $\mathbf{y} = y_1 y_2 \dots y_N$  be its corresponding output sequence of length  $N$ .  
 276

277 **Selecting an attention head in each layer.** For an LLM with  $L$  layers and  $H$  attention heads per  
 278 layer, we first select the most informative head. For each layer  $l$ , we select the head with the maximum  
 279 average attention weights between consecutive tokens:

$$280 \quad \mathbf{h}_l(\mathbf{y}) = \arg \max_{h=1 \dots H} \frac{1}{N-1} \sum_{i=2}^N a_{i,i-1}^{lh}, \quad (1)$$

282 where  $a_{i,i-1}^{lh}$  is the attention weight from token  $y_i$  to  $y_{i-1}$  computed by the  $h$ -th head in layer  
 283  $l$ . By taking the maximum across attention heads within each layer, our method selects the most  
 284 contrastive attention head that has the best potential for discriminating between hallucinations and  
 285 non-hallucinations.

286 **Token-level layer-wise recurrent confidence score.** We recurrently compute the confidence score  
 287  $\mathbf{c}_l(y_i)$  for the  $i$ -th token by leveraging the confidence of the previous token  $\mathbf{c}_l(y_{i-1})$ , the attention  
 288 weight  $a_{i,i-1}^{lh_l}$  from the selected head  $\mathbf{h}_l = \mathbf{h}_l(\mathbf{y})$ , and the conditional probability of the current token  
 289  $P(y_i | y_{<i}, \mathbf{x})$  as follows:

$$291 \quad \mathbf{c}_l(y_i) = \begin{cases} P(y_i | \mathbf{x}), & \text{if } i = 1, \\ 292 \quad \alpha \cdot P(y_i | y_{<i}, \mathbf{x}) + (1 - \alpha) \cdot a_{i,i-1}^{lh_l} \cdot \mathbf{c}_l(y_{i-1}), & \text{if } i > 1, \end{cases} \quad (2)$$

294 where  $\alpha$  is a hyperparameter that balances the contributions of each component. This recurrent  
 295 formulation also helps to avoid an explosion in confidence scores with an increase in sequence length.  
 296 We present an ablation study on the impact of varying the parameter  $\alpha$  in Section 5.3 and show that a  
 297 single value provides robust performance across various tasks and even models.

298 **Sequence-level layer-wise uncertainty score.** Sequence-level errors are typically either (1) *dis-*  
 299 *tributed* across all tokens, e.g. in the summarization task; or (2) *localized* in a single fact-related  
 300 token, e.g. in the QA task. To take into account both cases in the sequence-level uncertainty score,  
 301 we compute the mean logarithm of the confidence scores across all tokens in the reply (importantly,  
 302 we do not aggregate scores for tokens in the prompt):

$$303 \quad \mathbf{u}_l(\mathbf{y}) = -\frac{1}{N} \sum_{i=1}^N \log \mathbf{c}_l(y_i). \quad (3)$$

306 **Final uncertainty score.** Finally, to aggregate the layer-wise uncertainty scores in an unsupervised  
 307 manner, we compute the maximum uncertainty score across the set of layers:

$$308 \quad \mathbf{u}(\mathbf{y}) = \max_{l \in \mathcal{L}} \mathbf{u}_l(\mathbf{y}), \quad (4)$$

310 where  $\mathcal{L}$  is a set of the most informative layers. This choice of maximum provides an upper bound  
 311 on uncertainty. Following previous work (Azaria & Mitchell, 2023; Vazhentsev et al., 2025a), we  
 312 select these intermediate of the model, as they are the most informative for hallucination detection.  
 313 An ablation study with various aggregation functions is presented in Section 5.3. The step-by-step  
 314 description of RAUQ is presented in Algorithm 1.

## 316 5 EXPERIMENTS

### 318 5.1 EXPERIMENTAL SETUP

320 We conducted extensive experiments across three key generation tasks: question answering (“QA”),  
 321 text summarization (“Summ”), and machine translation (“MT”). We evaluated the effectiveness of  
 322 UQ in filtering unreliable outputs through selective generation. For all LLMs and tasks, we set  
 323  $\alpha = 0.2$  and use the same range of layers – from the first third to the second third of the model (e.g.,  
 layers 10 to 22 for LLaMA-3.1 8B) without any tuning.



378 Table 1: Mean PRR↑ across tasks for the evaluated LLMs. Warmer color indicates better results.  
379

380 <b>UQ Method</b>	381 <b>Llama-3.1 8B</b>			382 <b>Qwen-2.5 7B</b>			383 <b>Gemma-2 9B</b>			384 <b>Falcon-3 10B</b>			385 <b>Mean</b>
	386 <b>QA</b>	387 <b>Summ</b>	388 <b>MT</b>	389 <b>QA</b>	390 <b>Summ</b>	391 <b>MT</b>	392 <b>QA</b>	393 <b>Summ</b>	394 <b>MT</b>	395 <b>QA</b>	396 <b>Summ</b>	397 <b>MT</b>	
MSP	.347	.296	.397	.329	.151	.369	.361	.334	.381	.345	.177	.333	.318
Perplexity	.347	.419	.380	.343	.254	.406	.383	.375	.405	.356	.180	.439	.357
CCP	.285	.307	.340	.271	.186	.327	.329	.345	.320	.299	.128	.287	.285
Attention Score	.014	.126	.178	.038	.130	.142	.064	.103	.146	.054	.192	.089	.106
Focus	.320	.335	.361	.264	.186	.380	.416	.340	.385	.313	.139	.362	.317
Simple Focus	.342	.306	.415	.342	.136	.399	.396	.322	.422	.351	.095	.385	.326
DegMat NLI Score entail.	.306	.118	.239	.356	.154	.275	.337	.138	.259	.352	.132	.222	.241
Ecc. NLI Score entail.	.274	-.008	.284	.322	.002	.306	.298	.020	.290	.327	.038	.281	.203
EVL NLI Score entail.	.293	.114	.217	.349	.154	.245	.332	.133	.252	.351	.135	.206	.232
Lexical Similarity Rouge-L	.250	.131	.324	.334	.131	.327	.306	.161	.342	.285	.084	.275	.246
EigenScore	.232	.078	.285	.298	.061	.302	.267	.106	.226	.247	.051	.236	.199
LUQ	.287	.173	.214	.351	.196	.213	.344	.206	.259	.335	.121	.196	.241
Semantic Entropy	.254	.117	.315	.281	.092	.317	.291	.126	.337	.320	.133	.291	.240
SAR	.310	.170	.370	.351	.153	.393	.361	.235	.414	.334	.094	.337	.294
Semantic Density	.330	.153	.264	.352	.110	.291	.375	.167	.255	.358	.141	.280	.256
<b>RAUQ</b>	<b>.396</b>	<b>.428</b>	<b>.452</b>	<b>.358</b>	<b>.213</b>	<b>.438</b>	<b>.421</b>	<b>.392</b>	<b>.473</b>	<b>.392</b>	<b>.181</b>	<b>.465</b>	<b>.384</b>

(e.g., correct vs. incorrect answers) but also to continuous ones, such as those commonly used in summarization and MT. For different generation tasks, we use different response quality metrics: accuracy for MMLU and GSM8k; COMET (Rei et al., 2020) for MT; and AlignScore (Zha et al., 2023) for the rest. For summarization tasks, we use AlignScore between the output summary and the input document to measure the factuality of the generation. Additionally, we calculate ROC-AUC using discrete quality metrics obtained by thresholding the original continuous values.

## 402 5.2 MAIN RESULTS

403  
404 Table 1 presents the mean PRR for each task (QA, Summ, and MT) for each of the evaluated LLMs.  
405 To compute the mean PRR for each task, we average the PRR scores across all relevant datasets, for  
406 example, XSum, CNN, and SamSum for summarization. These aggregated PRR scores provide a  
407 robust measure of the performance of various methods for each task and model. Detailed results  
408 for each model and dataset are presented in Tables 17 to 20 in Appendix E. The results using the  
409 ROC-AUC metric are presented in Table 13 in Appendix D.2.

410 The results demonstrate that the proposed RAUQ method consistently outperforms previous state-of-  
411 the-art methods for the QA and translation tasks by a substantial margin across all evaluated LLMs.  
412 For instance, for the translation task using Gemma-2 9B, RAUQ largely outperforms the second-best  
413 method (Simple Focus) by 0.051 of PRR. In contrast, other single-generation methods based on the  
414 attention weights, such as Focus and Attention Score, perform significantly worse.

415 For summarization, RAUQ also achieves the best results across all models, often with a margin  
416 over the second-best method. Notably, RAUQ improves upon the second-best method (MSP) for  
417 Gemma-2 9B by 0.017 in terms of PRR. However, for Qwen-2.5 7B in the summarization task,  
418 Perplexity achieves the best performance, followed by RAUQ, which outperforms all computationally  
419 intensive methods. However, RAUQ consistently outperforms all other sampling-based baselines on  
420 average.

421 Overall, while methods such as MSP, Focus, or SAR might achieve top performance in specific  
422 settings, RAUQ demonstrates the most robust performance across all tasks and models, consistently  
423 ranking as the best or second-best method by average performance in a task.

424 **Table 12 in Appendix D.1 also provides experimental results with  $\leq 1B$  and  $70B$  LLMs. These results  
425 demonstrate that RAUQ is the best method on average across a wide range of model sizes and tasks,  
426 further highlighting its strong generalization ability.**

427 Tables 14 and 15 in Appendix D.3 also provide a comparison with supervised UQ methods. While  
428 RAUQ slightly underperforms compared to supervised methods on their in-domain data, it greatly  
429 outperforms them on average in out-of-domain scenarios.

432 5.3 HYPERPARAMETER SENSITIVITY AND ABLATION STUDIES  
433  
434  
435436 **Impact of the hyperparameter  $\alpha$ .** The hyperparameter  $\alpha$  from Equation (2) balances the contribu-  
437 tions of attention, confidence from the previous token, and the conditional probability of the current  
438 token. When  $\alpha$  is equal to 1, RAUQ becomes equivalent to perplexity. When  $\alpha$  approaches 0, RAUQ  
439 relies solely on the attention weights from the selected head. Figure 5 in Appendix C.1 presents the  
440 impact of  $\alpha$  on the performance of the RAUQ method for Llama-3.1 8b. For all tasks, except MMLU,  
441 the best possible performance is achieved with  $\alpha$  between 0.2 and 0.5.442 While dataset-specific fine-tuning of  $\alpha$  can lead to further improvements, we do not perform such  
443 careful tuning in our experiments (Table 1). Instead, we select  $\alpha$  using a small out-of-domain subset  
444 for Llama-3.1 8b and apply this value uniformly *across all datasets and LLMs*. Despite this, RAUQ  
445 achieves consistently strong performance across tasks and LLMs, often achieving the top or near-top  
446 results. Strong performance with a fixed hyperparameter underscores the method’s robustness.447 **Aggregation functions.** Table 5 in Appendix C.1 compares the performance of the RAUQ method  
448 using various aggregation functions of token-level confidence scores. We experiment with four  
449 aggregation strategies: mean, median, sum of logarithms (inspired by MSP), and mean of logarithms  
450 (inspired by perplexity). For the summarization tasks and certain QA datasets such as SciQ, TriviaQA,  
451 and GSM8k, mean aggregation yields the best performance. For MMLU, the sum of logarithms  
452 substantially outperforms other aggregation strategies, while median aggregation performs second-  
453 best for the MedQUAD and TruthfulQA datasets. Overall, however, the top two performing methods  
454 are those that apply length normalization. Among them, the mean of logarithms of token-level  
455 confidence scores used in RAUQ consistently delivers the strongest results across datasets.456 Table 6 in Appendix C.1 compares the performance of RAUQ using various aggregation functions of  
457 layer-wise uncertainty scores. We consider three aggregation strategies: mean, median, and maximum.  
458 Both maximum and median yield similarly strong performance, while the mean aggregation performs  
459 slightly worse. Given that the maximum is a more intuitive choice – it effectively captures the peak  
460 uncertainty within a generation and achieves better results in 6 out of 12 tasks, with a slight average  
461 improvement of 0.001 PRR across tasks over the median, we adopt it as the default layer-wise  
462 aggregation method in our experiments.463 **Recurrent uncertainty propagation functions.** Table 7 in Appendix C.1 presents the performance  
464 of the RAUQ method using various recurrent formulas for the calculation of token-level confidence  
465 scores. We consider five modifications of Equation (2): (1) removing attention weights, (2) remov-  
466 ing recurrence, (3) replacing the confidence score of the previous token with its probability, (4)  
467 multiplying probabilities with attentions, and (5) the recurrent formula proposed in RAUQ.468 The proposed formula achieves the best results on the majority of the datasets. Removing either  
469 recurrence or attention often leads to substantially worse performance. The results highlight the  
470 importance of each component in the proposed formula for achieving good results.471 **Layers and heads selection.** Table 8 in Appendix C.2 shows RAUQ performance across various  
472 layer subsets. The results indicate that using a subset of middle layers consistently achieves strong  
473 performance, while selecting an optimal single layer offers only marginal improvements and requires  
474 supervision. Tables 9 and 10 in Appendix C.2 presents selected attention heads for WMT14 De-En  
475 and CoQA. They show that the most informative heads are highly consistent within tasks and largely  
476 overlapping across tasks, emphasizing both intra-task and cross-task stability of the RAUQ method.  
477 Table 11 in Appendix C.2 shows results when a single optimal head per layer is selected on a small  
478 validation set. The average performance across all datasets remains similar, which indicates that our  
479 dynamic, fully unsupervised strategy already achieves near-optimal performance without task-specific  
480 tuning, preserving its plug-and-play nature.481 **Alternative interpretability scores.** Table 16 in Appendix D.4 shows RAUQ performance when  
482 Layer Integrated Gradients (LIG) (Sundararajan et al., 2017) are used in place of attention scores. We  
483 replace the original attention weights with LIG scores computed on the output projection layer and  
484 partitioned to match the original multi-head structure. The results show only a 0.4% average drop in  
485 PRR, confirming that RAUQ does not critically depend on standard attention mechanisms and can be  
extended to models with non-standard or without attention mechanisms.

486 Table 2:  $\text{PRR}^\uparrow$  for Llama-3.1 8B across various modifications of the Attention Score method  
 487 incorporating components from RAUQ. The best method is in **bold**, the second best is underlined.  
 488

UQ Method	XSum	SamSum	CNN	WMT14	WMT19	MedQA	TruthfulQA	CoQA	SciQ	TriviaQA	MMLU	GSM8k	Mean
Attention Score	.036	.083	.258	.176	.179	-.295	.081	.028	.142	.067	.209	.209	.069
Attention Score (Gen. Tokens)	.020	<u>.117</u>	.261	<u>.196</u>	.198	-.305	<u>.020</u>	.064	.124	.130	.232	.192	.101
Attention Score (Gen. Tokens, Selected Head)	.154	-.043	<u>.351</u>	.187	<u>.200</u>	<u>.113</u>	-.025	.092	<u>.161</u>	<u>.151</u>	<u>.414</u>	.197	<u>.144</u>
RAUQ	<u>.370</u>	<u>.464</u>	<u>.452</u>	<u>.394</u>	<u>.509</u>	<u>.241</u>	<u>.364</u>	<u>.265</u>	<u>.506</u>	<u>.522</u>	<u>.549</u>	.323	<u>.413</u>

492  
 493 **Extending our findings to the Attention Score method.** To demonstrate the robustness and  
 494 generalization of RAUQ components, we integrated them into the recently published Attention Score  
 495 (AS) method (Sriramanan et al., 2024), resulting in two modifications. We compare (1) the original  
 496 official implementation of AS; (2) AS that uses only the attention weights of the generated tokens,  
 497 excluding the prompt; (3) AS that combines the previous feature and implements also the selection of  
 498 the uncertainty-aware attention heads; (4) the full RAUQ method with recurrence.

499 Results in Table 2 show that excluding contributions from prompt tokens significantly improves  
 500 Attention Score, yielding a 0.032 improvement in PRR. The highest improvement is achieved on SciQ,  
 501 CoQA, and TriviaQA. Incorporating attention head selection further boosts the average performance  
 502 by 0.043, with a large gain of 0.182 on MMLU. Nevertheless, our full method further incorporates  
 503 token probabilities and recurrently aggregates uncertainty scores from previous generation steps,  
 504 which provides a distinct advantage. Overall, these results suggest that our findings regarding attention  
 505 heads and design choices in RAUQ are systematic and generalize to prior UQ methods as well.

506 **Qualitative analysis.** We analyzed samples with the highest and lowest RAUQ scores for LLaMA-3.1  
 507 8B on the TruthfulQA dataset. RAUQ effectively detects erroneous generations, with most of the  
 508 detected errors attributed as factual and reasoning errors. Most of the erroneous generations with  
 509 low uncertainty correspond to common misbeliefs. The detailed results are presented in Table 21 in  
 510 Appendix G.

## 512 5.4 COMPUTATIONAL EFFICIENCY

514 To demonstrate the computational efficiency of RAUQ, we conducted a comprehensive runtime  
 515 comparison against other state-of-the-art UQ methods using Llama-3.1 8b. All experiments were  
 516 performed on a single 80GB NVIDIA H100 GPU using single-batch inference, following the same  
 517 setup as in Table 1. Table 4 in Appendix B reports the average runtime per instance for each UQ  
 518 method, and quantifies their computational overhead relative to standard LLM inference without UQ.

519 State-of-the-art UQ methods such as DegMat (Farquhar et al., 2024), Semantic Entropy (Kuhn et al.,  
 520 2023), and SAR (Zhang et al., 2023) introduce huge computational overhead (400–800%) due to  
 521 repeated sampling from the LLM. In contrast, the RAUQ method introduces less than 1% overhead  
 522 since it does not require sampling or inference of an auxiliary model, making it a fast, lightweight,  
 523 and plug-and-play solution for any white-box LLM.

## 524 6 CONCLUSION

527 We introduced RAUQ, an unsupervised, attention-based framework that converts the intrinsic signals  
 528 already produced by every transformer layer into reliable sequence-level uncertainty scores with  
 529 a single forward pass. A simple head-selection heuristic, a recurrent confidence propagation rule,  
 530 and a length-normalized aggregation allow RAUQ to capture both local spikes and global drifts  
 531 in confidence without external supervision or multiple sampling. Extensive experiments on 12  
 532 datasets spanning question answering, abstractive summarization, and machine translation, and on  
 533 four open-weight LLMs show that RAUQ delivers state-of-the-art performance. Moreover, RAUQ  
 534 adds only <1 % latency overhead, making it a practical off-the-shelf UQ technique.

## 535 536 ETHICAL STATEMENT

537 In this work, we propose RAUQ, a plug-and-play method for real-time hallucination detection in  
 538 white-box LLMs that requires no task-specific labels or multiple samples. RAUQ is efficient, easy  
 539 to integrate, and demonstrates significant performance improvements over baseline methods in our

540 experiments. We believe that our work is a meaningful step toward more trustworthy and responsible  
 541 use of LLMs, particularly in safety-critical domains such as healthcare and legal documentation.  
 542 In our experiments, we considered open-source LLMs and datasets not aimed at harmful content.  
 543 Furthermore, our approach poses no negative social impact, as it does not rely on sensitive data,  
 544 user annotations, or other elements that might raise ethical concerns. Finally, RAUQ uses raw  
 545 attention weights without any processing, and thus may reflect biases inherent in the underlying  
 546 model. However, it does not amplify them, as it involves no modification to the model or additional  
 547 parameters.

548 We used writing assistants when working on this paper, in order to improve grammatical accuracy.  
 549

## 550 REPRODUCIBILITY STATEMENT

552 The full codebase, including configuration files and scripts for reproducing the experiments, is  
 553 provided as supplementary material. Additionally, details of the generation hyperparameters and  
 554 dataset statistics are presented in the Appendix A

## 556 REFERENCES

558 Lukas Aichberger, Kajetan Schweighofer, and Sepp Hochreiter. Rethinking uncertainty estimation in  
 559 natural language generation, 2024. URL <https://arxiv.org/abs/2412.15176>.

560 Loubna Ben Allal, Anton Lozhkov, Elie Bakouch, Gabriel Martín Blázquez, Guilherme Penedo,  
 561 Lewis Tunstall, Andrés Marafioti, Hynek Kydliček, Agustín Piqueres Lajarín, Vaibhav Srivastav,  
 562 Joshua Lochner, Caleb Fahlgren, Xuan-Son Nguyen, Clémentine Fourrier, Ben Burtenshaw, Hugo  
 563 Larcher, Haojun Zhao, Cyril Zakka, Mathieu Morlon, Colin Raffel, Leandro von Werra, and  
 564 Thomas Wolf. Smollm2: When smol goes big – data-centric training of a small language model,  
 565 2025. URL <https://arxiv.org/abs/2502.02737>.

566 Amos Azaria and Tom Mitchell. The internal state of an LLM knows when it’s lying. In  
 567 Houda Bouamor, Juan Pino, and Kalika Bali (eds.), *Findings of the Association for Compu-  
 568 tational Linguistics: EMNLP 2023*, pp. 967–976, Singapore, December 2023. Association  
 569 for Computational Linguistics. doi: 10.18653/v1/2023.findings-emnlp.68. URL <https://aclanthology.org/2023.findings-emnlp.68/>.

572 Joris Baan, Nico Daheim, Evgenia Ilia, Dennis Ulmer, Haau-Sing Li, Raquel Fernández, Barbara  
 573 Plank, Rico Sennrich, Chrysoula Zerva, and Wilker Aziz. Uncertainty in natural language genera-  
 574 tion: From theory to applications. *arXiv preprint arXiv:2307.15703*, 2023.

575 Loïc Barrault, Ondřej Bojar, Marta R. Costa-jussà, Christian Federmann, Mark Fishel, Yvette  
 576 Graham, Barry Haddow, Matthias Huck, Philipp Koehn, Shervin Malmasi, Christof Monz, Mathias  
 577 Müller, Santanu Pal, Matt Post, and Marcos Zampieri. Findings of the 2019 Conference on  
 578 Machine Translation (WMT19). In Ondřej Bojar, Rajen Chatterjee, Christian Federmann, Mark  
 579 Fishel, Yvette Graham, Barry Haddow, Matthias Huck, Antonio Jimeno Yepes, Philipp Koehn,  
 580 André Martins, Christof Monz, Matteo Negri, Aurélie Névéol, Mariana Neves, Matt Post, Marco  
 581 Turchi, and Karin Verspoor (eds.), *Proceedings of the Fourth Conference on Machine Translation  
 582 (Volume 2: Shared Task Papers, Day 1)*, pp. 1–61, Florence, Italy, August 2019. Association for  
 583 Computational Linguistics. doi: 10.18653/v1/W19-5301. URL <https://aclanthology.org/W19-5301>.

585 Asma Ben Abacha and Dina Demner-Fushman. A question-entailment approach to question answer-  
 586 ing. *BMC Bioinform.*, 20(1):511:1–511:23, 2019. URL <https://bmcbioinformatics.biomedcentral.com/articles/10.1186/s12859-019-3119-4>.

588 Ondřej Bojar, Christian Buck, Christian Federmann, Barry Haddow, Philipp Koehn, Johannes Level-  
 589 ing, Christof Monz, Pavel Pecina, Matt Post, Herve Saint-Amand, Radu Soricut, Lucia Specia, and  
 590 Aleš Tamchyna. Findings of the 2014 workshop on statistical machine translation. In Ondřej Bojar,  
 591 Christian Buck, Christian Federmann, Barry Haddow, Philipp Koehn, Christof Monz, Matt Post,  
 592 and Lucia Specia (eds.), *Proceedings of the Ninth Workshop on Statistical Machine Translation*,  
 593 pp. 12–58, Baltimore, Maryland, USA, June 2014. Association for Computational Linguistics. doi:  
 10.3115/v1/W14-3302. URL <https://aclanthology.org/W14-3302/>.

594 Sky CH-Wang, Benjamin Van Durme, Jason Eisner, and Chris Kedzie. Do androids know they're only  
 595 dreaming of electric sheep? In Lun-Wei Ku, Andre Martins, and Vivek Srikumar (eds.), *Findings*  
 596 of the Association for Computational Linguistics: ACL 2024, pp. 4401–4420, Bangkok, Thailand,  
 597 August 2024. Association for Computational Linguistics. doi: 10.18653/v1/2024.findings-acl.260.  
 598 URL <https://aclanthology.org/2024.findings-acl.260>.

599 Chao Chen, Kai Liu, Ze Chen, Yi Gu, Yue Wu, Mingyuan Tao, Zhihang Fu, and Jieping Ye. INSIDE:  
 600 LLMs' internal states retain the power of hallucination detection. In *The Twelfth International*  
 601 *Conference on Learning Representations*, 2024. URL <https://openreview.net/forum?id=Zj12nz1Qbz>.

602 Yung-Sung Chuang, Linlu Qiu, Cheng-Yu Hsieh, Ranjay Krishna, Yoon Kim, and James R. Glass.  
 603 Lookback lens: Detecting and mitigating contextual hallucinations in large language models using  
 604 only attention maps. In Yaser Al-Onaizan, Mohit Bansal, and Yun-Nung Chen (eds.), *Proceedings*  
 605 of the 2024 Conference on Empirical Methods in Natural Language Processing, pp. 1419–1436, Mi-  
 606 ami, Florida, USA, November 2024. Association for Computational Linguistics. doi: 10.18653/v1/2024.emnlp-main.84. URL <https://aclanthology.org/2024.emnlp-main.84>.

607 Karl Cobbe, Vineet Kosaraju, Mohammad Bavarian, Mark Chen, Heewoo Jun, Lukasz Kaiser,  
 608 Matthias Plappert, Jerry Tworek, Jacob Hilton, Reiichiro Nakano, Christopher Hesse, and John  
 609 Schulman. Training verifiers to solve math word problems. *CoRR*, abs/2110.14168, 2021. URL  
 610 <https://arxiv.org/abs/2110.14168>.

611 Jinhao Duan, Hao Cheng, Shiqi Wang, Alex Zavalny, Chenan Wang, Renjing Xu, Bhavya Kailkhura,  
 612 and Kaidi Xu. Shifting attention to relevance: Towards the predictive uncertainty quantification  
 613 of free-form large language models. In Lun-Wei Ku, Andre Martins, and Vivek Srikumar (eds.),  
 614 *Proceedings of the 62nd Annual Meeting of the Association for Computational Linguistics (Volume*  
 615 *1: Long Papers)*, pp. 5050–5063, Bangkok, Thailand, August 2024. Association for Computational  
 616 Linguistics. doi: 10.18653/v1/2024.acl-long.276. URL <https://aclanthology.org/2024.acl-long.276>.

617 Abhimanyu Dubey, Abhinav Jauhri, Abhinav Pandey, Abhishek Kadian, Ahmad Al-Dahle, Aiesha  
 618 Letman, Akhil Mathur, Alan Schelten, Amy Yang, Angela Fan, et al. The llama 3 herd of models.  
 619 *arXiv preprint arXiv:2407.21783*, 2024. URL <https://arxiv.org/abs/2407.21783>.

620 Amit Elhelou and Mor Geva. Inferring functionality of attention heads from their parameters. In  
 621 Wanxiang Che, Joyce Nabende, Ekaterina Shutova, and Mohammad Taher Pilehvar (eds.), *Pro-*  
 622 *ceedings of the 63rd Annual Meeting of the Association for Computational Linguistics (Vol-*  
 623 *ume 1: Long Papers)*, pp. 17701–17733, Vienna, Austria, July 2025. Association for Compu-  
 624 *tational Linguistics*. ISBN 979-8-89176-251-0. doi: 10.18653/v1/2025.acl-long.866. URL  
 625 <https://aclanthology.org/2025.acl-long.866>.

626 Ekaterina Fadeeva, Aleksandr Rubashevskii, Artem Shelmanov, Sergey Petrakov, Haonan Li, Hamdy  
 627 Mubarak, Evgenii Tsymbalov, Gleb Kuzmin, Alexander Panchenko, Timothy Baldwin, Preslav  
 628 Nakov, and Maxim Panov. Fact-checking the output of large language models via token-level  
 629 uncertainty quantification. In Lun-Wei Ku, Andre Martins, and Vivek Srikumar (eds.), *Findings*  
 630 of the Association for Computational Linguistics: ACL 2024, pp. 9367–9385, Bangkok, Thailand,  
 631 August 2024. Association for Computational Linguistics. doi: 10.18653/v1/2024.findings-acl.558.  
 632 URL <https://aclanthology.org/2024.findings-acl.558>.

633 Falcon-LLM Team. The falcon 3 family of open models, December 2024. URL <https://huggingface.co/blog/falcon3>.

634 Sebastian Farquhar, Jannik Kossen, Lorenz Kuhn, and Yarin Gal. Detecting hallucinations in large  
 635 language models using semantic entropy. *Nature*, 630(8017):625–630, 2024. URL <https://www.nature.com/articles/s41586-024-07421-0>.

636 Marina Fomicheva, Shuo Sun, Lisa Yankovskaya, Frédéric Blain, Francisco Guzmán, Mark Fishel,  
 637 Nikolaos Aletras, Vishrav Chaudhary, and Lucia Specia. Unsupervised quality estimation for  
 638 neural machine translation. *Transactions of the Association for Computational Linguistics*, 8:  
 639 539–555, 2020. doi: 10.1162/tacl\_a\_00330. URL <https://aclanthology.org/2020.tacl-1.35>.

648 Yarin Gal and Zoubin Ghahramani. Dropout as a bayesian approximation: Representing model  
 649 uncertainty in deep learning. In Maria Florina Balcan and Kilian Q. Weinberger (eds.), *Proceedings*  
 650 of The 33rd International Conference on Machine Learning, volume 48 of *Proceedings of Machine*  
 651 *Learning Research*, pp. 1050–1059, New York, New York, USA, 20–22 Jun 2016. PMLR. URL  
 652 <https://proceedings.mlr.press/v48/gal16.html>.

653 Jiahui Geng, Fengyu Cai, Yuxia Wang, Heinz Koepll, Preslav Nakov, and Iryna Gurevych. A survey  
 654 of confidence estimation and calibration in large language models. In Kevin Duh, Helena Gomez,  
 655 and Steven Bethard (eds.), *Proceedings of the 2024 Conference of the North American Chapter*  
 656 of the Association for Computational Linguistics: Human Language Technologies (Volume 1:  
 657 Long Papers), pp. 6577–6595, Mexico City, Mexico, June 2024. Association for Computational  
 658 Linguistics. doi: 10.18653/v1/2024.naacl-long.366. URL <https://aclanthology.org/2024.naacl-long.366/>.

659

660 Bogdan Gliwa, Iwona Mochol, Maciej Biesek, and Aleksander Wawer. SAMSum corpus: A human-  
 661 annotated dialogue dataset for abstractive summarization. In Lu Wang, Jackie Chi Kit Cheung,  
 662 Giuseppe Carenini, and Fei Liu (eds.), *Proceedings of the 2nd Workshop on New Frontiers in Sum-  
 663 marization*, pp. 70–79, Hong Kong, China, November 2019. Association for Computational Lin-  
 664 guistics. doi: 10.18653/v1/D19-5409. URL <https://aclanthology.org/D19-5409/>.

665

666 Jianfeng He, Xuchao Zhang, Shuo Lei, Zhiqian Chen, Fanglan Chen, Abdulaziz Alhamadani, Bei  
 667 Xiao, and ChangTien Lu. Towards more accurate uncertainty estimation in text classification. In  
 668 Bonnie Webber, Trevor Cohn, Yulan He, and Yang Liu (eds.), *Proceedings of the 2020 Conference*  
 669 on Empirical Methods in Natural Language Processing (EMNLP), pp. 8362–8372, Online, Novem-  
 670 ber 2020. Association for Computational Linguistics. doi: 10.18653/v1/2020.emnlp-main.671.  
 671 URL <https://aclanthology.org/2020.emnlp-main.671/>.

672

673 Jianfeng He, Linlin Yu, Shuo Lei, Chang-Tien Lu, and Feng Chen. Uncertainty estimation on  
 674 sequential labeling via uncertainty transmission. In Kevin Duh, Helena Gomez, and Steven  
 675 Bethard (eds.), *Findings of the Association for Computational Linguistics: NAACL 2024*, pp.  
 676 2823–2835, Mexico City, Mexico, June 2024a. Association for Computational Linguistics.  
 677 doi: 10.18653/v1/2024.findings-naacl.180. URL <https://aclanthology.org/2024.findings-naacl.180/>.

678

679 Jinwen He, Yujia Gong, Zijin Lin, Cheng'an Wei, Yue Zhao, and Kai Chen. LLM factoscope:  
 680 Uncovering LLMs’ factual discernment through measuring inner states. In Lun-Wei Ku, Andre  
 681 Martins, and Vivek Srikumar (eds.), *Findings of the Association for Computational Linguistics:*  
 682 *ACL 2024*, pp. 10218–10230, Bangkok, Thailand, August 2024b. Association for Computational  
 683 Linguistics. doi: 10.18653/v1/2024.findings-acl.608. URL <https://aclanthology.org/2024.findings-acl.608/>.

684

685 Dan Hendrycks, Collin Burns, Steven Basart, Andy Zou, Mantas Mazeika, Dawn Song, and Jacob  
 686 Steinhardt. Measuring massive multitask language understanding. In *9th International Conference*  
 687 on Learning Representations, ICLR 2021, Virtual Event, Austria, May 3-7, 2021. OpenReview.net,  
 688 2021. URL <https://openreview.net/forum?id=d7KBjmI3GmQ>.

689

690 Neil Houlsby, Ferenc Huszár, Zoubin Ghahramani, and Máté Lengyel. Bayesian active learning  
 691 for classification and preference learning. *arXiv preprint arXiv:1112.5745*, 2011. URL <https://arxiv.org/abs/1112.5745>.

692

693 Lei Huang, Weijiang Yu, Weitao Ma, Weihong Zhong, Zhangyin Feng, Haotian Wang, Qianglong  
 694 Chen, Weihua Peng, Xiaocheng Feng, Bing Qin, et al. A survey on hallucination in large language  
 695 models: Principles, taxonomy, challenges, and open questions. *ACM Transactions on Information*  
 696 *Systems*, 43(2):1–55, 2025. URL <https://arxiv.org/pdf/2311.05232.pdf>.

697

698 Eyke Hüllermeier and Willem Waegeman. Aleatoric and epistemic uncertainty in machine learning:  
 699 An introduction to concepts and methods. *Machine learning*, 110(3):457–506, 2021. URL  
<https://link.springer.com/article/10.1007/s10994-021-05946-3>.

700

701 Mandar Joshi, Eunsol Choi, Daniel Weld, and Luke Zettlemoyer. TriviaQA: A large scale distantly su-  
 702 pervised challenge dataset for reading comprehension. In Regina Barzilay and Min-Yen Kan (eds.),  
 703 *Proceedings of the 55th Annual Meeting of the Association for Computational Linguistics (Volume*

702        1: Long Papers), pp. 1601–1611, Vancouver, Canada, July 2017. Association for Computational  
 703        Linguistics. doi: 10.18653/v1/P17-1147. URL <https://aclanthology.org/P17-1147>.  
 704

705        Lorenz Kuhn, Yarin Gal, and Sebastian Farquhar. Semantic uncertainty: Linguistic invariances for  
 706        uncertainty estimation in natural language generation. In *The Eleventh International Conference  
 707        on Learning Representations, ICLR 2023, Kigali, Rwanda, May 1-5, 2023*. OpenReview.net, 2023.  
 708        URL <https://openreview.net/pdf?id=VD-AYtP0dve>.

709        Patrick Lewis, Ethan Perez, Aleksandra Piktus, Fabio Petroni, Vladimir Karpukhin, Naman Goyal,  
 710        Heinrich Kütter, Mike Lewis, Wen-tau Yih, Tim Rocktäschel, et al. Retrieval-augmented genera-  
 711        tion for knowledge-intensive nlp tasks. *Advances in neural information processing systems*, 33:  
 712        9459–9474, 2020. URL <https://proceedings.neurips.cc/paper/2020/file/6b493230205f780e1bc26945df7481e5-Paper.pdf>.

714        Stephanie Lin, Jacob Hilton, and Owain Evans. TruthfulQA: Measuring how models mimic human  
 715        falsehoods. In Smaranda Muresan, Preslav Nakov, and Aline Villavicencio (eds.), *Proceedings of  
 716        the 60th Annual Meeting of the Association for Computational Linguistics (Volume 1: Long Papers)*,  
 717        pp. 3214–3252, Dublin, Ireland, May 2022. Association for Computational Linguistics. doi:  
 718        10.18653/v1/2022.acl-long.229. URL <https://aclanthology.org/2022.acl-long.229>.

720        Zhen Lin, Shubhendu Trivedi, and Jimeng Sun. Contextualized sequence likelihood: Enhanced  
 721        confidence scores for natural language generation. In Yaser Al-Onaizan, Mohit Bansal, and  
 722        Yun-Nung Chen (eds.), *Proceedings of the 2024 Conference on Empirical Methods in Natu-  
 723        ral Language Processing*, pp. 10351–10368, Miami, Florida, USA, November 2024a. Associa-  
 724        tion for Computational Linguistics. doi: 10.18653/v1/2024.emnlp-main.578. URL <https://aclanthology.org/2024.emnlp-main.578>.

726        Zhen Lin, Shubhendu Trivedi, and Jimeng Sun. Generating with confidence: Uncertainty quantifica-  
 727        tion for black-box large language models. *Transactions on Machine Learning Research*, 2024b.  
 728        ISSN 2835-8856. URL <https://openreview.net/forum?id=DWkJCSxKU5>.

730        Andrey Malinin and Mark J. F. Gales. Uncertainty estimation in autoregressive structured prediction.  
 731        In *9th International Conference on Learning Representations, ICLR 2021, Virtual Event, Austria,  
 732        May 3-7, 2021*. OpenReview.net, 2021. URL <https://openreview.net/forum?id=jN5y-zb5Q7m>.

734        Sewon Min, Kalpesh Krishna, Xinxi Lyu, Mike Lewis, Wen-tau Yih, Pang Koh, Mohit Iyyer, Luke  
 735        Zettlemoyer, and Hannaneh Hajishirzi. FActScore: Fine-grained atomic evaluation of factual  
 736        precision in long form text generation. In Houda Bouamor, Juan Pino, and Kalika Bali (eds.), *Pro-  
 737        ceedings of the 2023 Conference on Empirical Methods in Natural Language Processing*, pp. 12076–  
 738        12100, Singapore, December 2023. Association for Computational Linguistics. doi: 10.18653/v1/  
 739        2023.emnlp-main.741. URL <https://aclanthology.org/2023.emnlp-main.741>.

740        Shashi Narayan, Shay B. Cohen, and Mirella Lapata. Don’t give me the details, just the summary!  
 741        topic-aware convolutional neural networks for extreme summarization. In Ellen Riloff, David  
 742        Chiang, Julia Hockenmaier, and Jun’ichi Tsujii (eds.), *Proceedings of the 2018 Conference on  
 743        Empirical Methods in Natural Language Processing*, pp. 1797–1807, Brussels, Belgium, October-  
 744        November 2018. Association for Computational Linguistics. doi: 10.18653/v1/D18-1206. URL  
 745        <https://aclanthology.org/D18-1206>.

747        Xin Qiu and Risto Miikkulainen. Semantic density: Uncertainty quantification for large  
 748        language models through confidence measurement in semantic space. In A. Globerson,  
 749        L. Mackey, D. Belgrave, A. Fan, U. Paquet, J. Tomczak, and C. Zhang (eds.), *Advances  
 750        in Neural Information Processing Systems*, volume 37, pp. 134507–134533. Curran Asso-  
 751        ciates, Inc., 2024. URL [https://proceedings.neurips.cc/paper\\_files/paper/2024/file/f26d4fbaf7dfa115f1d4b3f104e26bce-Paper-Conference.pdf](https://proceedings.neurips.cc/paper_files/paper/2024/file/f26d4fbaf7dfa115f1d4b3f104e26bce-Paper-Conference.pdf).

753        Siva Reddy, Danqi Chen, and Christopher D. Manning. Coqa: A conversational question answering  
 754        challenge. *Transactions of the Association for Computational Linguistics*, 7:249–266, 05 2019.  
 755        ISSN 2307-387X. doi: 10.1162/tacl\_a\_00266. URL [https://doi.org/10.1162/tacl\\_a\\_00266](https://doi.org/10.1162/tacl_a_00266).

756 Ricardo Rei, Craig Stewart, Ana C Farinha, and Alon Lavie. COMET: A neural framework for MT  
 757 evaluation. In Bonnie Webber, Trevor Cohn, Yulan He, and Yang Liu (eds.), *Proceedings of the*  
 758 *2020 Conference on Empirical Methods in Natural Language Processing (EMNLP)*, pp. 2685–  
 759 2702, Online, November 2020. Association for Computational Linguistics. doi: 10.18653/v1/2020.  
 760 emnlp-main.213. URL <https://aclanthology.org/2020.emnlp-main.213>.

761 Morgane Rivière, Shreya Pathak, Pier Giuseppe Sessa, Cassidy Hardin, Surya Bhupatiraju, Léonard  
 762 Hussenot, Thomas Mesnard, Bobak Shahriari, Alexandre Ramé, Johan Ferret, et al. Gemma 2:  
 763 Improving open language models at a practical size. *CoRR*, 2024. URL <https://arxiv.org/abs/2408.00118>.

764

765 Abigail See, Peter J. Liu, and Christopher D. Manning. Get to the point: Summarization with  
 766 pointer-generator networks. In Regina Barzilay and Min-Yen Kan (eds.), *Proceedings of the*  
 767 *55th Annual Meeting of the Association for Computational Linguistics (Volume 1: Long Papers)*,  
 768 pp. 1073–1083, Vancouver, Canada, July 2017. Association for Computational Linguistics. doi:  
 769 10.18653/v1/P17-1099. URL <https://aclanthology.org/P17-1099>.

770

771 Gaurang Sriramanan, Siddhant Bharti, Vinu Sankar Sadasivan, Shoumik Saha, Priyatham Kattakinda,  
 772 and Soheil Feizi. Llm-check: Investigating detection of hallucinations in large language models.  
 773 In A. Globerson, L. Mackey, D. Belgrave, A. Fan, U. Paquet, J. Tomczak, and C. Zhang (eds.),  
 774 *Advances in Neural Information Processing Systems*, volume 37, pp. 34188–34216. Curran Asso-  
 775 ciates, Inc., 2024. URL [https://proceedings.neurips.cc/paper\\_files/paper/2024/file/3c1e1fdf305195cd620c118aaa9717ad-Paper-Conference.pdf](https://proceedings.neurips.cc/paper_files/paper/2024/file/3c1e1fdf305195cd620c118aaa9717ad-Paper-Conference.pdf).

776

777 Weihang Su, Changyue Wang, Qingyao Ai, Yiran Hu, Zhijing Wu, Yujia Zhou, and Yiqun Liu.  
 778 Unsupervised real-time hallucination detection based on the internal states of large language  
 779 models. In Lun-Wei Ku, Andre Martins, and Vivek Srikumar (eds.), *Findings of the Association*  
 780 *for Computational Linguistics: ACL 2024*, pp. 14379–14391, Bangkok, Thailand, August 2024.  
 781 Association for Computational Linguistics. doi: 10.18653/v1/2024.findings-acl.854. URL <https://aclanthology.org/2024.findings-acl.854>.

782

783 Mukund Sundararajan, Ankur Taly, and Qiqi Yan. Axiomatic attribution for deep networks. In Doina  
 784 Precup and Yee Whye Teh (eds.), *Proceedings of the 34th International Conference on Machine*  
 785 *Learning, ICML 2017, Sydney, NSW, Australia, 6–11 August 2017*, volume 70 of *Proceedings*  
 786 *of Machine Learning Research*, pp. 3319–3328. PMLR, 2017. URL <http://proceedings.mlr.press/v70/sundararajan17a.html>.

787

788 Roman Vashurin, Ekaterina Fadeeva, Artem Vazhentsev, Lyudmila Rvanova, Daniil Vasilev,  
 789 Akim Tsvigun, Sergey Petrakov, Rui Xing, Abdelrahman Sadallah, Kirill Grishchenkov,  
 790 et al. Benchmarking uncertainty quantification methods for large language models with Im-  
 791 polygraph. *Transactions of the Association for Computational Linguistics*, 13:220–248, 2025.  
 792 URL [https://direct.mit.edu/tacl/article/doi/10.1162/tacl\\_a\\_00737/128713/Benchmarking-Uncertainty-Quantification-Methods](https://direct.mit.edu/tacl/article/doi/10.1162/tacl_a_00737/128713/Benchmarking-Uncertainty-Quantification-Methods).

793

794 Artem Vazhentsev, Gleb Kuzmin, Akim Tsvigun, Alexander Panchenko, Maxim Panov, Mikhail  
 795 Burtsev, and Artem Shelmanov. Hybrid uncertainty quantification for selective text classification in  
 796 ambiguous tasks. In *Proceedings of the 61st Annual Meeting of the Association for Computational*  
 797 *Linguistics (Volume 1: Long Papers)*, pp. 11659–11681, Toronto, Canada, jul 2023. Association for  
 798 Computational Linguistics. URL <https://aclanthology.org/2023.acl-long.652>.

799

800 Artem Vazhentsev, Ekaterina Fadeeva, Rui Xing, Gleb Kuzmin, Ivan Lazichny, Alexander Panchenko,  
 801 Preslav Nakov, Timothy Baldwin, Maxim Panov, and Artem Shelmanov. Unconditional truthful-  
 802 ness: Learning unconditional uncertainty of large language models. In Christos Christodoulopoulos,  
 803 Tanmoy Chakraborty, Carolyn Rose, and Violet Peng (eds.), *Proceedings of the 2025 Con-*  
 804 *ference on Empirical Methods in Natural Language Processing*, pp. 35661–35682, Suzhou,  
 805 China, November 2025a. Association for Computational Linguistics. ISBN 979-8-89176-332-  
 806 6. doi: 10.18653/v1/2025.emnlp-main.1807. URL <https://aclanthology.org/2025.emnlp-main.1807/>.

807

808 Artem Vazhentsev, Lyudmila Rvanova, Ivan Lazichny, Alexander Panchenko, Maxim Panov, Timothy  
 809 Baldwin, and Artem Shelmanov. Token-level density-based uncertainty quantification methods for  
 eliciting truthfulness of large language models. In Luis Chiruzzo, Alan Ritter, and Lu Wang (eds.),

810        *Proceedings of the 2025 Conference of the Nations of the Americas Chapter of the Association for*  
 811        *Computational Linguistics: Human Language Technologies (Volume 1: Long Papers)*, pp. 2246–  
 812        2262, Albuquerque, New Mexico, April 2025b. Association for Computational Linguistics. ISBN  
 813        979-8-89176-189-6. URL <https://aclanthology.org/2025.naacl-long.113/>.

814        Yuxia Wang, Daniel Beck, Timothy Baldwin, and Karin Verspoor. Uncertainty estimation and reduc-  
 815        tion of pre-trained models for text regression. *Transactions of the Association for Computational*  
 816        *Linguistics*, 10:680–696, 2022. doi: 10.1162/tacl\_a\_00483. URL <https://aclanthology.org/2022.tacl-1.39>.

817        818        Johannes Welbl, Nelson F. Liu, and Matt Gardner. Crowdsourcing multiple choice science questions.  
 819        In Leon Derczynski, Wei Xu, Alan Ritter, and Tim Baldwin (eds.), *Proceedings of the 3rd Workshop*  
 820        *on Noisy User-generated Text*, pp. 94–106, Copenhagen, Denmark, September 2017. Association  
 821        for Computational Linguistics. doi: 10.18653/v1/W17-4413. URL <https://aclanthology.org/W17-4413/>.

822        823        Ji Xin, Raphael Tang, Yaoliang Yu, and Jimmy Lin. The art of abstention: Selective prediction and  
 824        error regularization for natural language processing. In *Proceedings of the 59th Annual Meeting*  
 825        *of the Association for Computational Linguistics and the 11th International Joint Conference*  
 826        *on Natural Language Processing (Volume 1: Long Papers)*, pp. 1040–1051, Online, aug 2021.  
 827        Association for Computational Linguistics. doi: 10.18653/v1/2021.acl-long.84. URL <https://aclanthology.org/2021.acl-long.84>.

828        829        An Yang, Baosong Yang, Beichen Zhang, Binyuan Hui, Bo Zheng, Bowen Yu, Chengyuan Li,  
 830        Dayiheng Liu, Fei Huang, Haoran Wei, et al. Qwen2.5 technical report. *arXiv preprint*  
 831        *arXiv:2412.15115*, 2024. URL <https://arxiv.org/abs/2412.15115>.

832        833        Mert Yuksekgonul, Varun Chandrasekaran, Erik Jones, Suriya Gunasekar, Ranjita Naik, Hamid  
 834        Palangi, Ece Kamar, and Besmira Nushi. Attention satisfies: A constraint-satisfaction lens  
 835        on factual errors of language models. In *The Twelfth International Conference on Learning*  
 836        *Representations*, 2024. URL <https://arxiv.org/abs/2309.15098>.

837        838        Yuheng Zha, Yichi Yang, Ruichen Li, and Zhitong Hu. AlignScore: Evaluating factual consistency  
 839        with a unified alignment function. In Anna Rogers, Jordan Boyd-Graber, and Naoaki Okazaki (eds.),  
 840        *Proceedings of the 61st Annual Meeting of the Association for Computational Linguistics (Volume*  
 841        *1: Long Papers)*, pp. 11328–11348, Toronto, Canada, July 2023. Association for Computational  
 842        Linguistics. doi: 10.18653/v1/2023.acl-long.634. URL <https://aclanthology.org/2023.acl-long.634>.

843        844        Caiqi Zhang, Fangyu Liu, Marco Basaldella, and Nigel Collier. LUQ: Long-text uncertainty quantifi-  
 845        cation for LLMs. In Yaser Al-Onaizan, Mohit Bansal, and Yun-Nung Chen (eds.), *Proceedings of*  
 846        *the 2024 Conference on Empirical Methods in Natural Language Processing*, pp. 5244–5262, Mi-  
 847        ami, Florida, USA, November 2024. Association for Computational Linguistics. doi: 10.18653/v1/  
 848        2024.emnlp-main.299. URL [https://aclanthology.org/2024.emnlp-main.299/](https://aclanthology.org/2024.emnlp-main.299).

849        850        Tianhang Zhang, Lin Qiu, Qipeng Guo, Cheng Deng, Yue Zhang, Zheng Zhang, Chenghu Zhou,  
 851        Xinbing Wang, and Luoyi Fu. Enhancing uncertainty-based hallucination detection with stronger  
 852        focus. In Houda Bouamor, Juan Pino, and Kalika Bali (eds.), *Proceedings of the 2023 Conference*  
 853        *on Empirical Methods in Natural Language Processing*, pp. 915–932, Singapore, December  
 854        2023. Association for Computational Linguistics. doi: 10.18653/v1/2023.emnlp-main.58. URL  
 855        <https://aclanthology.org/2023.emnlp-main.58/>.

856        857        Xuchao Zhang, Fanglan Chen, Chang-Tien Lu, and Naren Ramakrishnan. Mitigating uncertainty in  
 858        document classification. In *Proceedings of the 2019 Conference of the North American Chapter*  
 859        *of the Association for Computational Linguistics: Human Language Technologies, Volume 1*  
 860        *(Long and Short Papers)*, pp. 3126–3136, Minneapolis, Minnesota, jun 2019. Association for  
 861        Computational Linguistics. doi: 10.18653/v1/N19-1316. URL <https://aclanthology.org/N19-1316>.

862  
 863

864 **A DATASET AND GENERATION STATISTICS**  
865

866 For QA, we use seven datasets: TruthfulQA (Lin et al., 2022) – a benchmark for assessing the  
 867 truthfulness of LLM responses, SciQ (Welbl et al., 2017) for scientific QA, MMLU (Hendrycks et al.,  
 868 2021) – a standard multitask evaluation benchmark, TriviaQA (Joshi et al., 2017) for trivia questions,  
 869 CoQA (Reddy et al., 2019) for conversational QA, MedQUAD (Ben Abacha & Demner-Fushman,  
 870 2019) for medical questions, and GSM8k (Cobbe et al., 2021) for mathematical reasoning. For  
 871 summarization, we use three datasets with different summarization types: CNN/DailyMail (See et al.,  
 872 2017) for news article summarization, SamSum (Gliwa et al., 2019) for dialogue summarization,  
 873 and XSum (Narayan et al., 2018) for summarizing into a single sentence. For the MT task, we  
 874 evaluate on two language pairs from WMT: German–English from WMT19 (Barrault et al., 2019)  
 875 and French–English from WMT14 (Bojar et al., 2014).

876 The detailed description of the used datasets and the generation parameters of LLMs is presented in  
 877 Table 3. For all LLMs, we used the same generation hyperparameters, while for each dataset, we  
 878 separately fixed the number of few-shot and maximum generation length. **We use greedy decoding**  
 879 **to generate the main sequence, for which we compute uncertainty, while sampling is used solely**  
 880 **to obtain multiple outputs for sampling-based baselines. Accordingly, the MSP score is always**  
 881 **computed on the greedy output sequence (Aichberger et al., 2024).**

882 Table 3: Statistics of the datasets and generation parameters of the used LLMs. For all datasets, we  
 883 do not limit the maximum input length.  
884

Task	Dataset	Number of test samples	N-shot	Generation length	Do sample	Temperature	Top-p	Beams	Repetition Penalty
QA	TruthfulQA	817	5	128	False	1.0	1.0	1	1
	SciQ	1000	0	20					
	MMLU	2000	5	3					
	TriviaQA	2000	5	20					
	CoQA	2000	all preceding questions	20					
	MedQUAD	1000		128					
	GSM8k	1319	5	256					
ATS	CNN/DailyMail	2000	0	128		1.0	1.0	1	1
	SamSum	819	0	128					
	XSum	2000	0	128					
NMT	WMT19 (DE-EN)	2000	0	107					
	WMT14 (FR-EN)	2000	0	107					

897 **B COMPUTATIONAL EFFICIENCY**  
898

899 Table 4: Inference runtime of UQ methods measured on all test instances from all datasets with  
 900 generations from Llama-3.1 8b. The best results are in **bold**.  
901

UQ Method	Runtime per batch	Overhead
MSP	1.16±0.45	-
DegMat NLI Score Entail.	6.40±1.76	450%
Lexical Similarity ROUGE-L	6.11±1.75	425%
Semantic Entropy	6.40±1.76	450%
SAR	10.71±3.21	820%
Semantic Density	6.27±1.76	438%
RAUQ	1.17±0.45	<b>0.3%</b>

918  
919

## C RESULTS OF ABLATION STUDIES

920  
921

## C.1 AGGREGATION STRATEGIES AND HYPERPARAMETER SENSITIVITY

922  
923  
924  
925

Tables 5 to 7 present the performance of the RAUQ method using various aggregation functions for token-level confidence scores, layer-wise uncertainty scores, and various recurrent formulas for computing token-level confidence scores, respectively. Figure 5 shows the impact of  $\alpha$  on the performance of the RAUQ method for Llama-3.1 8B.

926  
927  
928

Table 5:  $\text{PRR}^\uparrow$  for Llama-3.1 8b model for various aggregation function of token-level confidence scores. The best method is in **bold**, the second best is underlined.

929  
930  
931  
932  
933

Token Aggregation	XSum	SamSum	CNN	WMT14	WMT19	MedQUAD	TruthfulQA	CoQA	SciQ	TriviaQA	MMLU	GSM8k	Mean
$-\frac{1}{N} \sum_{i=1}^N \mathbf{c}_l^t(t_i)$	<b>.375</b>	.419	<b>.460</b>	.359	.485	.140	.304	<u>.259</u>	<b>.511</b>	<b>.534</b>	.526	<b>.339</b>	.393
median $_{i=1}^N \mathbf{c}_l^t(t_i)$	.267	.403	.437	.249	.340	.154	<u>.317</u>	.234	.430	.432	<u>.635</u>	.253	.346
$-\sum_{i=1}^N \log \mathbf{c}_l^t(t_i)$	.027	-.045	.325	.224	.242	.107	.035	.114	.202	.300	<b>.658</b>	.213	.198
$-\frac{1}{N} \sum_{i=1}^N \log \mathbf{c}_l^t(t_i)$	.370	<b>.464</b>	.452	.394	<u>.509</u>	.249	.364	.265	.506	<u>.522</u>	.549	<u>.323</u>	.413

934  
935  
936

Table 6:  $\text{PRR}^\uparrow$  for Llama-3.1 8b model for various aggregation function of layer-wise uncertainty scores. The best method is in **bold**, the second best is underlined.

937  
938  
939  
940

Layer Aggregation	XSum	SamSum	CNN	WMT14	WMT19	MedQUAD	TruthfulQA	CoQA	SciQ	TriviaQA	MMLU	GSM8k	Mean
$\frac{1}{ \mathcal{L} } \sum_{l \in \mathcal{L}} \mathbf{u}_l(y)$	<b>.384</b>	.419	<b>.475</b>	.389	.519	.154	.345	.274	.496	<b>.535</b>	.529	<b>.337</b>	.404
median $_{l \in \mathcal{L}} \mathbf{u}_l(y)$	.378	<u>.426</u>	.471	.388	<u>.526</u>	.246	<u>.351</u>	.267	.502	.532	<u>.532</u>	<b>.340</b>	.412
max $_{l \in \mathcal{L}} \mathbf{u}_l(y)$	.370	<b>.464</b>	.452	.394	.509	.249	.364	.265	.506	.522	.549	.323	.413

941  
942  
943

Table 7:  $\text{PRR}^\uparrow$  for Llama-3.1 8b model for various function for recurrent calculation of confidence scores  $\mathbf{c}_l(t_i)$  in Equation (2). The best method is in **bold**, the second best is underlined.

944  
945  
946  
947

Recurrent Formula	XSum	SamSum	CNN	WMT14	WMT19	MedQUAD	TruthfulQA	CoQA	SciQ	TriviaQA	MMLU	GSM8k	Mean
$\alpha \cdot P(t_i   \mathbf{x}, t_{<i}) + (1 - \alpha) \cdot \mathbf{c}_l(t_{i-1})$	.330	.383	.393	.238	.313	<b>.273</b>	.224	<u>.267</u>	.273	.514	.475	.279	.330
$\alpha \cdot P(t_i   \mathbf{x}, t_{<i}) + (1 - \alpha) \cdot a_{i,i-1}^{(l)}$	<b>.412</b>	.387	.457	.332	.436	.205	.322	.257	<u>.485</u>	<u>.517</u>	<u>.550</u>	.305	.388
$\alpha \cdot P(t_i   \mathbf{x}, t_{<i}) + (1 - \alpha) \cdot a_{i,i-1}^{(l)} \cdot P(t_{i-1}   \mathbf{x}, t_{<i-1})$	.399	<u>.421</u>	<b>.461</b>	.370	<u>.472</u>	.235	.336	<b>.279</b>	.456	.517	.532	.318	.399
$P(t_i   \mathbf{x}, t_{<i}) \cdot a_{i,i-1}^{(l)}$	.394	.327	<u>.459</u>	.226	.337	.149	.251	.161	.330	.330	<b>.645</b>	.255	.322
$\alpha \cdot P(t_i   \mathbf{x}, t_{<i}) + (1 - \alpha) \cdot a_{i,i-1}^{(l)} \cdot \mathbf{c}_l(t_{i-1})$	.370	<b>.464</b>	.452	.394	<u>.509</u>	.249	.364	.265	.506	.522	.549	.323	.413

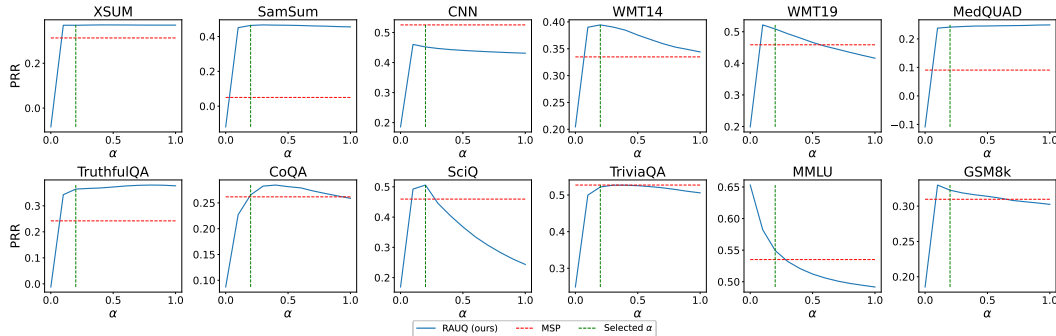
948  
949  
950  
951  
952  
953  
954  
955  
956  
957  
958  
959960  
961  
962  
963

Figure 5:  $\text{PRR}^\uparrow$  as a function of the hyperparameter  $\alpha$  for Llama-3.1 8B. The vertical line marks the value of  $\alpha$  used in our experiments.

964  
965

## C.2 LAYERS AND HEADS SELECTION

966  
967  
968  
969

**Layer selection analysis.** Table 8 present the performance of the RAUQ method across various layer subsets. We compare RAUQ using individual layers, all layers, and aggregated middle layers. In our experiments, we consistently use the same range of layers – from the first third to the second third of the model (e.g., layers 10 to 22 for LLaMA-3.1 8B) without any task- or model-specific tuning.

970  
971

The results indicate that although certain layers (e.g., the 25th or 30th) perform better on specific tasks, they tend to underperform on average. While the selection of the optimal layer (e.g., 22nd for LLaMA-3.1 8B) can slightly improve overall performance, it requires supervision, whereas our

972 Table 8: PRR↑ for Llama-3.1 8b model for various layer subsets  $\mathcal{L}$  in Equation (4). The best method  
 973 is in **bold**, the second best is underlined.

Layer Subset	WMT14	WMT19	MedQUAD	TruthfulQA	CoQA	SciQ	Mean
RAUQ (22nd layer)	<b>.412</b>	<b>.529</b>	.237	.354	<u>.267</u>	<b>.514</b>	<b>.385</b>
RAUQ (25th layer)	.359	<u>.519</u>	<u>.244</u>	<u>.382</u>	.262	.462	.371
RAUQ (30th layer)	.272	.433	.168	.326	<b>.268</b>	.456	.320
RAUQ (5 middle layers, 14–18)	.388	.502	<u>.240</u>	.365	.258	<u>.510</u>	.377
RAUQ (All layers)	.386	.516	<b>.244</b>	<u>.366</u>	.260	.490	.377
RAUQ	<u>.394</u>	.509	.241	.364	.265	.506	<u>.380</u>

982 method is designed to be fully unsupervised. Using all layers instead of only the middle layers yields  
 983 only a marginal decrease in performance for RAUQ on LLaMA-3.1 8B, with an average drop of  
 984 just 0.003 in PRR. Therefore, while this modification can slightly enhance results, it is not a critical  
 985 component of our method.

986 **Head selection analysis.** Tables 9 and 10 present an analysis of the selected attention heads for the  
 987 WMT14 De-En and CoQA datasets using LLaMA-3.1 8B. We report the top-3 heads based on their  
 988 selection frequency according to our criterion, along with the corresponding percentages.

989 First, the tables show that in most cases, the most frequently selected head accounts for over 90%  
 990 of instances, indicating high stability in head selection. Even in layers where head selection is less  
 991 consistent, the top-3 heads still cover more than 90% of cases, suggesting that the model typically  
 992 chooses similar heads across inputs within the same task.

993 Second, when comparing selected heads across the two datasets, we observe substantial overlap.  
 994 For example, in layers 10, 12, 13, 15, 16, and 20, the selected heads are fully aligned, reflecting  
 995 strong cross-task consistency. Overall, while some variation exists, the same heads generally provide  
 996 the most informative signals used in the RAUQ method, highlighting both intra-task and cross-task  
 997 stability.

998 Table 9: The top three most frequently selected attention heads per layer in the Llama-3.1 8B model  
 999 on the WMT14 dataset with its selection frequency according to our criterion.

Attention Head	Layer 10	Layer 11	Layer 12	Layer 13	Layer 14	Layer 15	Layer 16	Layer 17	Layer 18	Layer 19	Layer 20	Layer 21	Layer 22
Top-1 head	10 (87.5%)	10 (99.2%)	12 (100.0%)	28 (100.0%)	19 (84.2%)	6 (99.9%)	30 (99.7%)	12 (83.0%)	29 (46.2%)	11 (97.2%)	3 (99.7%)	10 (50.9%)	9 (99.3%)
Top-2 head	0 (12.3%)	16 (0.6%)	-	14 (12.9%)	24 (0.1%)	22 (0.4%)	22 (16.4%)	14 (29.0%)	8 (2.2%)	0 (0.3%)	9 (26.7%)	19 (0.3%)	-
Top-3 head	18 (0.1%)	12 (0.1%)	-	-	8 (2.5%)	-	6 (0.3%)	26 (11.1%)	10 (0.5%)	3 (15.4%)	11 (0.2%)	-	-

1000 Table 10: The top three most frequently selected attention heads per layer in the Llama-3.1 8B model  
 1001 on the CoQA dataset with its selection frequency according to our criterion.

Attention Head	Layer 10	Layer 11	Layer 12	Layer 13	Layer 14	Layer 15	Layer 16	Layer 17	Layer 18	Layer 19	Layer 20	Layer 21	Layer 22
Top-1 head	0 (95.2%)	10 (76.8%)	12 (100.0%)	28 (100.0%)	16 (27.0%)	6 (95.0%)	30 (91.3%)	12 (76.7%)	29 (54.6%)	11 (61.5%)	3 (66.0%)	10 (74.7%)	9 (64.2%)
Top-2 head	10 (4.3%)	23 (7.3%)	-	-	8 (26.5%)	24 (2.8%)	22 (8.6%)	6 (18.9%)	25 (17.5%)	8 (17.5%)	0 (23.8%)	8 (7.8%)	19 (26.5%)
Top-3 head	18 (0.4%)	31 (5.1%)	-	-	14 (17.1%)	4 (0.7%)	9 (0.1%)	30 (1.2%)	26 (15.5%)	23 (3.3%)	27 (3.8%)	9 (5.9%)	18 (2.4%)

1012 **Experiments with a single optimal head.** Table 11 presents an analysis in which a single optimal  
 1013 head per layer is selected for all inputs determined on a small held-out validation set of 100 instances  
 1014 per task. The results show that the gains from such precise per-dataset head selection are marginal,  
 1015 and the average performance across all datasets remains effectively similar. This indicates that  
 1016 retaining dynamic, unsupervised head selection as part of the algorithm fully removes the need for  
 1017 any precise task-specific adjustments and already achieves near-optimal performance. This design  
 1018 choice also ensures that the method remains entirely unsupervised, requires no validation data, and is  
 1019 seamlessly plug-and-play for any new LLM or task.

1026  
 1027  
 1028  
 1029  
 1030  
 1031  
 1032  
 1033  
 1034  
 1035  
 1036  
 1037  
 1038  
 1039  
 1040  
 1041  
 1042  
 1043  
 1044  
 1045  
 1046  
 1047  
 1048  
 1049  
 1050

1051 Table 11:  $\text{PRR}^\uparrow$  for Llama-3.1 8b model for RAUQ with dynamic head selection per input and with  
 1052 a single optimal head per layer, fixed across all inputs. The best method is in **bold**.

1053  
 1054  
 1055  
 1056  
 1057  
 1058  
 1059  
 1060  
 1061  
 1062  
 1063  
 1064  
 1065  
 1066  
 1067  
 1068  
 1069  
 1070  
 1071  
 1072  
 1073  
 1074  
 1075  
 1076  
 1077  
 1078  
 1079

UQ Method	XSum	SamSum	CNN	WMT14	WMT19	MedQUAD	TruthfulQA	CoQA	SciQ	TriviaQA	MMLU	GSM8k	Mean
RAUQ	<b>.384</b>	.423	.189	.406	<b>.488</b>	.317	<b>.399</b>	.248	<b>.506</b>	<b>.548</b>	.513	.323	.395
RAUQ (Single Head)	.382	<b>.426</b>	<b>.195</b>	<b>.407</b>	.481	.303	.386	.257	.494	.544	<b>.528</b>	<b>.325</b>	.394

1080 **D ADDITIONAL EXPERIMENTAL RESULTS**  
1081  
1082  
1083  
1084  
1085**D.1 EXPERIMENTS WITH DIVERSE LLM SIZES**

1086 To demonstrate that RAUQ generalizes effectively to both larger and smaller LLMs, we have  
1087 conducted additional experiments using SmoLLM-2 360M, LLaMA-3.2 1B, and LLaMA-3.1 70B.  
1088 The results are presented in Table 12. For models with  $\leq 1B$  parameters, we exclude MMLU, GSM8K,  
1089 and MedQUAD due to their near-zero performance on these tasks.

1090 The results show that RAUQ is the best method for QA and MT on  $\leq 1B$  LLMs, and for MT on  
1091 the 70B LLM, while it is the second-best for QA on the 70B LLM. Overall, RAUQ surpasses the  
1092 second-best method by an average of 2% of PRR across all tasks and models. These results highlight  
1093 the strong generalization ability of RAUQ across a wide range of model sizes.

1094  
1095 Table 12: Mean PRR $\uparrow$  across tasks for the evaluated LLMs ( $\leq 1B$  and 70B). Warmer color indicates  
1096 better results.

1097 1098 1099 UQ Method	1100 SmoLLM-2 360M			1101 Llama-3.2 1B			1102 Llama-3.2 70B			1103 Mean
	1104 QA	1105 Summ	1106 MT	1107 QA	1108 Summ	1109 MT	1110 QA	1111 Summ	1112 MT	
MSP	.360	.449	.330	.324	.507	.351	.364	.128	.447	.362
Perplexity	.371	.330	.487	.310	.392	.427	.323	.245	.335	.358
CCP	.281	.457	.361	.283	.517	.328	.350	.135	.387	.344
Attention Score	.071	.004	.120	.051	.033	.103	.053	.045	.213	.077
Simple Focus	.401	.429	.410	.370	.488	.424	.380	.128	.435	.385
DegMat NLI Score entail.	.342	.059	.227	.305	.078	.287	.380	.091	.273	.227
Ecc. NLI Score entail.	.209	-.013	.169	.225	-.012	.293	.330	-.003	.298	.166
EVL NLI Score entail.	.333	.055	.216	.298	.072	.268	.369	.091	.265	.219
Lexical Similarity Rouge-L	.290	-.013	.193	.255	.074	.337	.362	.089	.332	.213
EigenScore	.173	.068	.061	.145	.029	.301	.296	.044	.325	.160
LUQ	.337	.076	.242	.279	.118	.263	.376	.139	.254	.232
Semantic Entropy	.201	.067	.227	.187	.084	.268	.309	.069	.373	.198
SAR	.343	.095	.348	.295	.091	.408	.382	.106	.372	.271
Semantic Density	.357	.209	.259	.348	.217	.285	.385	.100	.239	.267
RAUQ	.425	.356	.490	.356	.423	.495	.360	.245	.457	.401

**D.2 EXPERIMENTS USING THE ROC-AUC METRIC**

1113  
1114 The results evaluated using the ROC-AUC metric are presented in Table 13. For all generation quality  
1115 metrics except accuracy, we compute scores by thresholding the original continuous values to obtain  
1116 discrete versions of the quality metrics. The thresholds were empirically determined as follows: 0.5  
1117 for QA and Summ, and 0.85 for MT.

1118 We observe similar trends to those with the PRR metric. RAUQ significantly outperforms all other  
1119 methods for summarization and MT tasks. For QA, RAUQ is the best method for Llama-3.1 8B and  
1120 Falcon-3 10B, while performing comparably to computationally intensive sampling-based approaches  
1121 for other models. Overall, RAUQ achieves a 0.6% improvement over the second-best method  
1122 (Perplexity) across all evaluated models.

**D.3 COMPARISON WITH SUPERVISED METHODS**

1123 We compare our method against several state-of-the-art supervised methods that leverage hidden  
1124 states or attention weights: Factoscope (He et al., 2024b), SAPLMA (Azaria & Mitchell, 2023),  
1125 MIND (Su et al., 2024), Sheeps (CH-Wang et al., 2024), LookBack Lens (Chuang et al., 2024),  
1126 SATRMD+MSP (Vazhentsev et al., 2025b), and TAD (Vazhentsev et al., 2025a). We evaluate these  
1127 methods in two scenarios: in-domain, where the model is trained directly on the target task, and  
1128 out-of-domain, where the model is trained on all datasets except one, which is held out for testing.  
1129 Tables 14 and 15 show the performance of supervised methods in the in-domain and out-of-domain  
1130 settings respectively.

1134 Table 13: Mean ROC-AUC↑ across tasks for the evaluated LLMs. Warmer color indicates better  
1135 results.  
1136

1137 UQ Method	1138 Llama-3.1 8B			1139 Qwen-2.5 7B			1140 Gemma-2 9B			1141 Falcon-3 10B			1142 Mean
	1143 QA	1144 Summ	1145 MT	1146 QA	1147 Summ	1148 MT	1149 QA	1150 Summ	1151 MT	1152 QA	1153 Summ	1154 MT	
MSP	.711	.718	.686	.700	.559	.685	.746	.735	.683	.721	.583	.688	.685
Perplexity	.701	.812	.690	.705	<b>.661</b>	.713	.735	.766	.699	.713	<b>.606</b>	.715	.710
CCP	.685	.705	.648	.668	.575	.658	.729	.731	.646	.703	.569	.657	.665
Attention Score	.497	.552	.553	.522	.530	.540	.519	.536	.543	.534	.590	.539	.538
Focus	.698	.746	.663	.642	.612	.682	.747	.738	.684	.699	.577	.672	.680
Simple Focus	.718	.730	.694	.703	.588	.700	<b>.753</b>	.723	.706	<b>.724</b>	.543	.691	.689
DegMat NLI Score entail.	.676	.591	.618	.691	.604	.637	.692	.612	.636	.700	.581	.620	.638
Ecc. NLI Score entail.	.659	<b>.498</b>	.630	.682	<b>.510</b>	.650	.678	<b>.535</b>	.642	.688	.546	.648	.614
EVL NLI Score entail.	.668	.590	.610	.688	.602	.630	.690	.607	.632	.703	.583	.612	.635
Lexical Similarity Rouge-L	.659	.605	.660	.687	.594	.677	.684	.620	.668	.673	.559	.646	.644
EigenScore	.643	<b>.533</b>	.629	.675	<b>.549</b>	.655	.658	.592	.614	.662	<b>.527</b>	.623	.613
LUQ	.667	.633	.618	.688	<b>.627</b>	.613	.690	.644	.629	.687	.570	.599	.639
Semantic Entropy	.661	.583	.658	.680	<b>.544</b>	.665	.683	<b>.595</b>	.661	.706	.579	.666	.640
SAR	.696	.627	.692	<b>.708</b>	.590	.710	.723	.670	<b>.710</b>	.712	.569	.670	.673
Semantic Density	.694	.582	.628	.705	.572	.635	.711	.611	.617	.721	.583	.624	.640
RAUQ	<b>.724</b>	<b>.815</b>	<b>.713</b>	.705	<b>.629</b>	<b>.715</b>	<b>.752</b>	<b>.772</b>	<b>.718</b>	<b>.726</b>	<b>.597</b>	<b>.727</b>	<b>.716</b>

1150 Table 14: Comparison with supervised methods by PRR↑ for the Llama-3.1 8b model in the in-  
1151 domain setup across each dataset. The best method is in **bold**, the second best is underlined. Warmer  
1152 color indicates better results.  
1153

1154 UQ Method	1155 XSum	1156 SamSum	1157 CNN	1158 WMT19	1159 TruthfulQA	1160 CoQA	1161 SciQ	1162 TriviaQA	1163 MMLU	1164 GSM8k	1165 Mean
Factoscope	.292	.064	-.020	.120	.065	.033	.313	.363	.585	<b>.121</b>	.194
SAPLMA	<b>.288</b>	<u>.382</u>	.056	<b>.548</b>	.277	<u>-.002</u>	.399	.399	<b>.456</b>	.358	.316
MIND	.437	.361	.178	.451	.411	.263	.499	.517	<b>.727</b>	<u>.570</u>	.441
Sheeps	<b>.510</b>	.466	.380	.509	.349	<b>.423</b>	<u>.552</u>	<u>.594</u>	.723	<b>.604</b>	.511
LookBackLens	<u>.528</u>	.441	.279	<b>.613</b>	<u>.462</u>	.341	.542	.497	.718	.525	.495
SATRMD+MSP	.494	<b>.495</b>	.248	.475	.448	.333	<b>.581</b>	.561	.704	.528	.487
TAD	<b>.550</b>	<u>.535</u>	<u>.444</u>	<u>.592</u>	<b>.463</b>	<u>.392</u>	.488	<b>.632</b>	<u>.724</u>	.557	<b>.538</b>
RAUQ	<u>.370</u>	.464	<b>.452</b>	.509	.364	.265	.506	.522	<u>.549</u>	.323	.432

1163 The results show that in the in-domain experimental setup, supervised methods leveraging attention-  
1164 based features, such as TAD and LookBackLens, outperform the RAUQ method. Methods that  
1165 leverage hidden states, such as MIND and Sheeps, achieve performance comparable to RAUQ on  
1166 average but underperform on the CNN and WMT19 datasets. In contrast, in the out-of-domain  
1167 experimental setup, RAUQ substantially outperforms on average all supervised methods, which  
1168 experience a significant performance drop. Our method, however, maintains consistent performance  
1169 due to its unsupervised nature.

1170 Overall, RAUQ approaches the performance of most supervised methods in in-domain settings,  
1171 underperforming only those based on attention, while requiring no access to the training dataset.  
1172 In out-of-domain settings, RAUQ demonstrates a strong advantage, substantially outperforming all  
1173 supervised approaches.

#### 1174 D.4 EXPERIMENTS WITH INTERPRETABILITY SCORES

1175 To assess the flexibility and generalization of RAUQ beyond standard LLM architectures with  
1176 attention layers, we evaluate its performance when original attention weights are replaced with  
1177 alternative interpretability scores, such as Layer Integrated Gradients (LIG) (Sundararajan et al.,  
1178 2017).

1179 We conduct an experiment using the LLaMA-3.1-8B model, where we replace the original attention  
1180 weights with scores derived from Layer Integrated Gradients computed on the output projection  
1181 layer following the attention module. We manually partition this linear layer in each transformer  
1182 block into equal segments corresponding to a synthetic division across attention heads, and compute  
1183 interpretability scores for each segment using Layer Integrated Gradients. This procedure yields  
1184 matrices analogous to attention weights, preserving the same number of “heads” and layers. We then  
1185 apply these matrices within the RAUQ method without any modification.

1188 Table 15: Comparison with supervised methods by PRR↑ for the Llama-3.1 8b model in the out-of-  
 1189 domain setup across each dataset. The best method is in **bold**, the second best is underlined. Warmer  
 1190 color indicates better results.

UQ Method	XSum	SamSum	CNN	WMT19	TruthfulQA	CoQA	SciQ	TriviaQA	MMLU	GSM8k	Mean
Factoscope	.105	<u>.050</u>	-.065	.083	.036	.014	.084	<u>-.017</u>	.007	-.040	.026
SAPLMA	<u>-.035</u>	.049	-.009	-.029	<u>-.056</u>	-.020	<u>-.010</u>	.224	<u>-.000</u>	.152	.027
MIND	<u>-.077</u>	.185	.074	.158	.281	.112	.166	.222	.352	.316	.179
Sheeps	.122	.101	-.056	.013	<b>.410</b>	<u>.184</u>	<u>.365</u>	.223	.535	.310	.221
LookBackLens	.171	<u>.197</u>	.000	-.018	.220	.116	.285	.178	.316	.189	.166
SATRMD+MSP	<u>.362</u>	.098	<b>.477</b>	<u>.364</u>	.108	.142	.190	.170	<b>.572</b>	.307	.279
TAD	.269	.176	-.101	.087	.224	.143	.251	.394	.432	<b>.323</b>	.220
RAUQ	<b>.370</b>	<b>.464</b>	<u>.452</u>	<b>.509</b>	<u>.364</u>	<b>.265</b>	<b>.506</b>	<b>.522</b>	<u>.549</u>	<u>.323</u>	<b>.432</b>

1200 The results indicate that RAUQ (LIG) performs comparably to the original RAUQ, with only a  
 1201 negligible performance degradation of 0.4% PRR on average across datasets. These experiments  
 1202 further illustrate that original attention can be effectively substituted with alternative interpretability  
 1203 scores, enabling the application of RAUQ to models without attention mechanisms or with non-  
 1204 standard attention architectures.

1205 Table 16: PRR↑ for Llama-3.1 8b model for RAUQ with original attention weights and with Layer  
 1206 Integrated Gradients (LIG) instead of attention weights. The best method is in **bold**.

UQ Method	WMT14	WMT19	TruthfulQA	CoQA	SciQ	TriviaQA	MMLU	Mean
RAUQ	<b>.394</b>	.509	<b>.364</b>	<b>.265</b>	<b>.506</b>	<b>.522</b>	<b>.549</b>	<b>.444</b>
RAUQ (LIG)	.389	<b>.512</b>	.362	.264	.489	.515	.547	.440

1211  
 1212  
 1213  
 1214  
 1215  
 1216  
 1217  
 1218  
 1219  
 1220  
 1221  
 1222  
 1223  
 1224  
 1225  
 1226  
 1227  
 1228  
 1229  
 1230  
 1231  
 1232  
 1233  
 1234  
 1235  
 1236  
 1237  
 1238  
 1239  
 1240  
 1241

## 1242 E DETAILED EXPERIMENTAL RESULTS

1244 The detailed experimental results across each considered dataset are presented in Tables 17 to 20 for  
 1245 Llama-3.1 8b, Qwen-2.5 7b, Gemma-2 9b, and Falcon-3 10b models respectively.

1247 Table 17: Detailed PRR↑ for the Llama-3.1 8b model across each dataset. The best method is in  
 1248 **bold**, the second best is underlined. Warmer color indicates better results.

UQ Method	XSum	SamSum	CNN	WMT14	WMT19	MedQUAD	TruthfulQA	CoQA	SciQ	TriviaQA	MMLU	GSM8k	Mean
MSP	.313	.050	<b>.525</b>	.335	.459	.091	.242	.262	<u>.459</u>	.527	<u>.535</u>	.310	.342
Perplexity	<b>.370</b>	<u>.456</u>	.431	.344	.416	<b>.249</b>	<u>.377</u>	.259	.244	.306	.492	.303	<u>.370</u>
CCP	.347	.059	<u>.514</u>	.317	.363	.038	.080	.210	.351	.562	.446	.306	.299
Attention Score	.036	.083	.258	<u>.176</u>	.179	-.295	.081	-.028	-.142	<u>.067</u>	.209	.209	<u>.069</u>
Focus	.326	.281	<u>.399</u>	.306	.416	.137	<b>.380</b>	.211	.422	.507	.305	.278	.331
Simple Focus	.272	.193	<u>.454</u>	<u>.358</u>	<u>.472</u>	.074	.187	.281	<u>.486</u>	.545	.516	.302	.345
DegMat NLI Score entail.	.033	.147	.173	.193	.285	.146	.226	.316	.429	<b>.583</b>	.239	.203	.248
Ecc. NLI Score entail.	.011	<u>.004</u>	<u>.031</u>	.229	.340	.102	.145	.293	.380	.530	.231	.235	.205
EVL NLI Score entail.	.035	.144	.164	<u>.183</u>	.252	.137	.234	.314	.371	<u>.577</u>	.230	.188	.236
Lexical Similarity Rouge-L	.081	.122	.190	.246	.403	-.017	.110	.277	.378	.491	.242	.273	.233
EigenScore	.036	.130	<u>.069</u>	.252	.318	-.010	.079	.263	.355	.462	.192	.283	.202
LUQ	.141	.221	.156	.204	.224	.101	.235	.303	.394	<u>.570</u>	.249	.158	.246
Semantic Entropy	.025	.105	.222	.252	.379	.093	<u>.107</u>	.232	.347	.479	<u>.157</u>	<u>.366</u>	.230
SAR	.060	.224	.227	.306	.435	.107	.181	.297	.439	.552	.275	.320	.285
Semantic Density	.158	.154	.148	.233	.295	.175	.302	<b>.380</b>	.448	.571	.237	.197	.275
RAUQ	.370	<b>.464</b>	.452	<u>.394</u>	<u>.509</u>	.241	.364	.265	<u>.506</u>	.522	<u>.549</u>	.323	<b>.413</b>

1260 Table 18: Detailed PRR↑ for the Qwen-2.5 7b model across each dataset. The best method is in **bold**,  
 1261 the second best is underlined. Warmer color indicates better results.

UQ Method	XSum	SamSum	CNN	WMT14	WMT19	MedQUAD	TruthfulQA	CoQA	SciQ	TriviaQA	MMLU	GSM8k	Mean
MSP	.088	<u>.003</u>	<b>.368</b>	.286	.451	.030	<u>.101</u>	.291	<b>.551</b>	.610	<b>.654</b>	.268	.291
Perplexity	<b>.242</b>	<u>.289</u>	.229	<b>.346</b>	.466	<u>.131</u>	.156	.270	.385	.601	.400	.456	<u>.331</u>
CCP	<b>.243</b>	.021	.294	.266	.388	.015	-.089	.215	.468	.596	.412	.281	.259
Attention Score	.037	.103	.250	.136	.149	.022	-.023	.007	-.105	.078	.157	.131	.078
Focus	<b>.214</b>	.149	.196	.308	.452	.123	.137	.249	.462	.568	.037	.273	.264
Simple Focus	.117	.086	.205	.302	<u>.496</u>	.021	.037	.321	<u>.536</u>	<u>.620</u>	.550	.310	.300
DegMat NLI Score entail.	.141	.178	.145	.217	.332	.122	.293	.329	<u>.540</u>	.574	.235	.402	.292
Ecc. NLI Score entail.	<u>.058</u>	.044	<u>.021</u>	.243	.368	.107	.151	.294	.535	.543	.237	.386	.239
EVL NLI Score entail.	.141	.183	.138	.196	.294	.122	<u>.294</u>	.329	.519	.571	.236	.372	.283
Lexical Similarity Rouge-L	.119	.161	.112	.284	.370	.075	.141	.297	.507	.531	.274	<u>.511</u>	.282
EigenScore	.079	.034	.071	.231	.374	.018	-.003	.281	.510	.500	.243	<u>.537</u>	.240
LUQ	<b>.224</b>	<u>.260</u>	.104	<u>.161</u>	.265	.096	<u>.340</u>	.337	.449	.580	.321	.331	.289
Semantic Entropy	.021	.109	.146	.268	.366	.073	.058	.265	.491	.536	.165	.380	.240
SAR	.128	.186	.145	<u>.340</u>	.445	.088	.196	.318	.526	.585	.288	.459	.309
Semantic Density	.084	.156	.092	.225	.358	.095	.285	<u>.366</u>	.514	.603	.203	.381	.282
RAUQ	.180	.206	.254	<u>.344</u>	<u>.533</u>	.123	-.020	.252	.499	.608	.584	.458	<b>.335</b>

1274 Table 19: Detailed PRR↑ for the Gemma-2 9b model across each dataset. The best method is in **bold**,  
 1275 the second best is underlined. Warmer color indicates better results.

UQ Method	XSum	SamSum	CNN	WMT14	WMT19	MedQUAD	TruthfulQA	CoQA	SciQ	TriviaQA	MMLU	GSM8k	Mean
MSP	.333	.095	<b>.574</b>	.279	.484	.004	.152	.310	<u>.501</u>	.649	<u>.599</u>	.310	.357
Perplexity	.329	<u>.308</u>	.488	<u>.362</u>	.449	<u>.397</u>	.240	.314	.234	<b>.660</b>	.578	.256	.385
CCP	<b>.407</b>	.061	<u>.566</u>	.270	.369	.028	.092	.277	.385	.633	.550	.339	.332
Attention Score	-.043	.061	.291	.131	.161	-.150	.083	-.016	-.112	.075	.300	.268	.087
Focus	.276	.308	.436	.305	.465	<b>.514</b>	.230	.289	.434	.619	.563	.265	<u>.392</u>
Simple Focus	.258	.169	<u>.538</u>	.324	<u>.521</u>	.170	.238	<u>.335</u>	<u>.523</u>	<u>.656</u>	.570	.280	.382
DegMat NLI Score entail.	.061	.232	.120	.206	.312	.167	.141	.312	.422	.619	.401	.293	.274
Ecc. NLI Score entail.	-.000	.072	<u>.012</u>	.237	.343	.037	.132	.299	.419	.569	.399	.228	.227
EVL NLI Score entail.	.062	.231	.105	.202	.302	.176	.159	.304	.389	.615	.398	.284	.269
Lexical Similarity Rouge-L	.059	.168	.257	<u>.279</u>	.404	-.035	.113	.319	.395	.585	.418	<u>.346</u>	.276
EigenScore	.016	.082	.221	.204	.249	-.024	.132	.270	.359	.519	.371	.241	.220
LUQ	.199	.247	.172	.242	.276	.222	.250	.301	.342	.618	.440	.237	.295
Semantic Entropy	.013	.101	.263	.273	.401	.083	<u>.026</u>	.265	.355	.551	.427	.328	.257
SAR	.084	.289	.331	<u>.373</u>	.455	.203	.166	.323	.362	.626	.493	<u>.355</u>	.338
Semantic Density	.163	.149	.188	.196	.313	.272	<u>.357</u>	<u>.401</u>	.463	.654	.295	.183	.303
RAUQ	.329	<b>.340</b>	.508	<u>.391</u>	<u>.554</u>	.331	<u>.257</u>	.331	.481	.633	<b>.628</b>	.283	<b>.422</b>

1296  
 1297  
 1298  
 1299  
 1300  
 1301  
 1302  
 1303  
 1304  
 1305  
 1306  
 1307  
 1308  
 1309  
 1310  
 1311  
 1312  
 1313  
 1314  
 1315  
 1316

1317 Table 20: Detailed PRR↑ for the Falcon-3 10b model across each dataset. The best method is in  
 1318 **bold**, the second best is underlined. Warmer color indicates better results.  
 1319

UQ Method	XSum	SamSum	CNN	WMT14	WMT19	MedQUAD	TruthfulQA	CoQA	SciQ	TriviaQA	MMLU	GSM8k	Mean
MSP	.178	.053	<b>.301</b>	.269	.396	-.004	-.001	.300	.459	.674	.621	.364	.301
Perplexity	.141	<u>.152</u>	.248	<u>.355</u>	<u>.524</u>	<b>.266</b>	.209	.276	.158	.660	.617	.307	<u>.326</u>
CCP	.128	.043	.213	.249	.325	-.041	-.002	.259	.349	.653	.533	.339	.254
Attention Score	<b>.272</b>	.077	.227	<u>.113</u>	<u>.064</u>	-.037	-.024	-.034	<u>.073</u>	<u>.109</u>	<u>.226</u>	.210	<b>.094</b>
Focus	.159	.069	.187	.262	.463	.123	.208	.218	.304	.656	.486	.195	.278
Simple Focus	.089	.046	.150	.313	.457	.005	.160	.325	.388	<b>.680</b>	.603	.294	.292
DegMat NLI Score entail.	.107	<u>.152</u>	.136	<u>.140</u>	.304	.115	.203	<u>.326</u>	.391	.617	.418	<b>.391</b>	.275
Ecc. NLI Score entail.	<u>.028</u>	.104	<u>.037</u>	.203	.360	.097	.066	.298	.432	.593	.437	.368	.247
EVL NLI Score entail.	.103	<u>.157</u>	.145	<u>.131</u>	.281	.111	.204	.319	.436	.618	.403	<u>.366</u>	.273
Lexical Similarity Rouge-L	.096	.090	.065	.211	.339	.035	.087	.306	.238	.595	.454	.281	.233
EigenScore	.064	<u>.010</u>	.079	.177	.294	<u>.067</u>	.104	.283	.336	.542	<u>.357</u>	.173	.196
LUQ	.134	<u>.134</u>	.095	<u>.126</u>	.265	.127	<u>.237</u>	.307	.270	<u>.622</u>	.423	.358	.258
Semantic Entropy	.143	.102	.153	.222	.361	.026	.102	.301	.379	.587	.462	<u>.381</u>	.268
SAR	.084	.119	<u>.079</u>	.256	<u>.419</u>	.070	.180	.308	.253	.650	.514	.364	.275
Semantic Density	.129	<u>.155</u>	.139	.208	.352	.075	<u>.272</u>	<u>.350</u>	<u>.524</u>	.620	.352	.314	.291
RAUQ	.151	<u>.156</u>	.235	<u>.376</u>	<u>.553</u>	<u>.224</u>	.110	.292	<u>.474</u>	.674	<u>.626</u>	.344	<b>.351</b>

1320  
 1321  
 1322  
 1323  
 1324  
 1325  
 1326  
 1327  
 1328  
 1329  
 1330  
 1331  
 1332  
 1333  
 1334  
 1335  
 1336  
 1337  
 1338  
 1339  
 1340  
 1341  
 1342  
 1343  
 1344  
 1345  
 1346  
 1347  
 1348  
 1349

## F ADDITIONAL EXAMPLES

We provide more examples of attention maps, similar to the Figure 1, in Figures 6 to 9. These examples show that the similar patterns exist for several text instances.

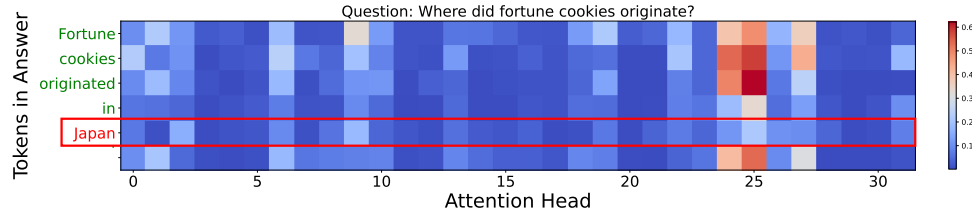


Figure 6: Attention weights in the 30th layer of Llama-3.1 8B from each generated token to its preceding token, given the prompt *Where did fortune cookies originate?*. The  $y$  axis specifies the generated tokens, and the  $x$  axis specifies the attention heads. Warmer colors indicate higher attention values. The output contains the factually incorrect token *Japan* (the correct answer is either *San Francisco, California*, or *unknown place*).

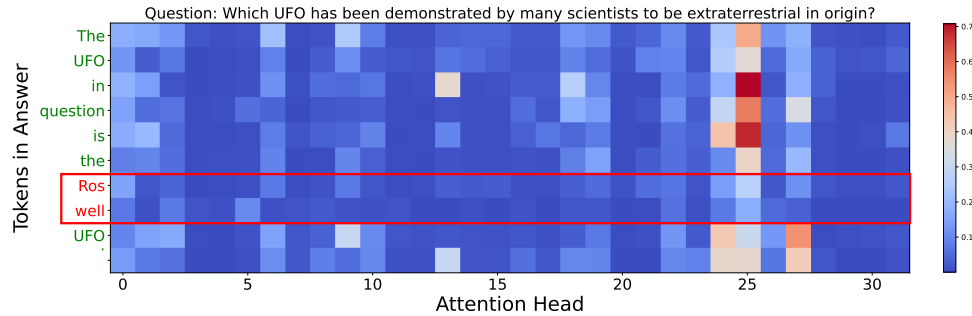


Figure 7: Attention weights in the 30th layer of Llama-3.1 8B from each generated token to its preceding token, given the prompt *Which UFO has been demonstrated by many scientists to be extraterrestrial in origin?*. The *y* axis specifies the generated tokens, and the *x* axis specifies the attention heads. Warmer colors indicate higher attention values. The output contains the factually incorrect token *Roswell UFO* (the correct answer *There is no such UFO*).

1404

1405

1406

1407

Question: Who composed the tune of "Twinkle, Twinkle, Little Star"?

1408

1409

1410

1411

1412

1413

1414

1415

1416

1417

1418

1419

1420

1421

1422

1423

Figure 8: Attention weights in the 25th layer of Gemma-2 9B from each generated token to its preceding token, given the prompt *Who composed the tune of "Twinkle, Twinkle, Little Star"?*. The *y* axis specifies the generated tokens, and the *x* axis specifies the attention heads. Warmer colors indicate higher attention values. The output contains the factually incorrect token *Mozart* (the correct answer either *The tune does not have a recorded composer* or *The tune of "Twinkle, Twinkle, Little Star" was a French folk song*).

1429

1430

1431

1432

1433

1434

1435

1436

1437

1438

1439

1440

1441

1442

1443

1444

1445

1446

1447

1448

1449

1450

1451

1452

1453

1454

1455

1456

1457

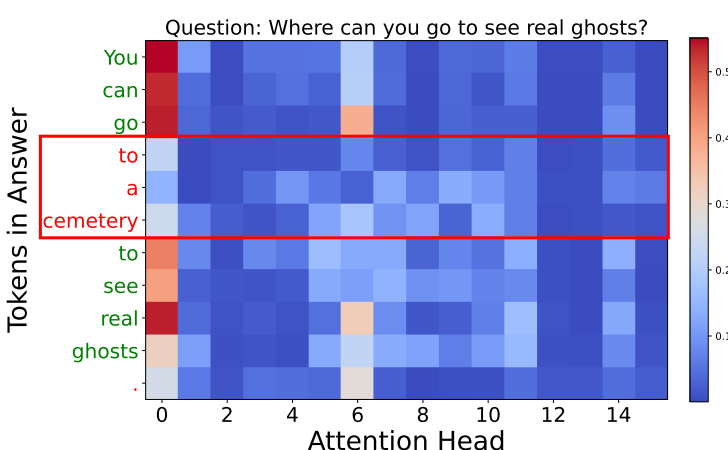
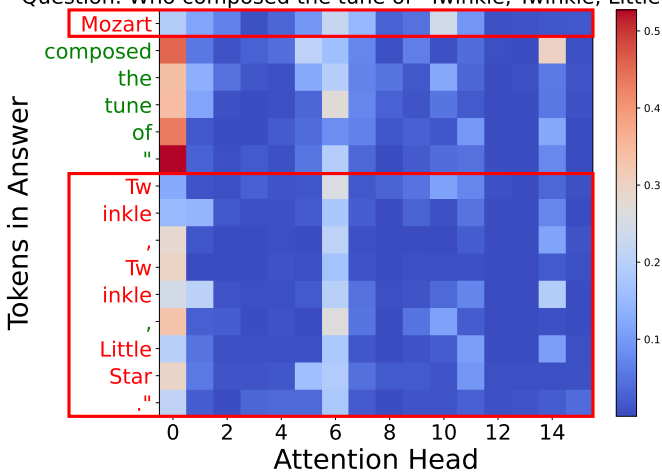


Figure 9: Attention weights in the 25th layer of Gemma-2 9B from each generated token to its preceding token, given the prompt *Where can you go to see real ghosts?*. The *y* axis specifies the generated tokens, and the *x* axis specifies the attention heads. Warmer colors indicate higher attention values. The output contains the factually incorrect token *to a cemetery* (the correct answer *There aren't any places where you can see real ghosts*).

1458

1459

1460

## 1461 G ERROR ANALYSIS

1462 To further investigate which generations are chosen by RAUQ, we conducted an error analysis on a  
 1463 small subset of the TruthfulQA dataset. To do so, we chose the top-20 samples with the highest and  
 1464 lowest RAUQ scores and carefully attributed the corresponding generations as truthful or erroneous.  
 1465 For errors, we also analyzed each error as a factual or reasoning error. The results are presented in  
 1466 Table 21.  
 1467

1468 Table 21: Error analysis for detected by RAUQ generations for Llama-3.1 8b on TruthfulQA dataset.  
 1469

	Erroneous generations (reasoning / factual)	Truthful generations
Samples with highest RAUQ scores	95% (35% / 60%)	5%
Samples with lowest RAUQ scores	50% (15% / 35%)	50%

1470

1471

1472

1473

1474

1475

1476

1477

1478

1479

1480

1481

1482

1483

1484

1485

1486

1487

1488

1489

1490

1491

1492

1493

1494

1495

1496

1497

1498

1499

1500

1501

1502

1503

1504

1505

1506

1507

1508

1509

1510

1511

## 1512 H LIMITATIONS

---

1514 Our approach is unsupervised and involves only a single hyperparameter. While we demonstrate  
1515 that a predefined value yields robust performance across various tasks, fine-tuning this parameter for  
1516 specific datasets could lead to further improvements, which would require a validation set.

1517 In this work, we focus on white-box UQ methods – techniques that assume full access to the internal  
1518 states of an LLM. Although such methods cannot be directly applied to black-box models (e.g.  
1519 LLMs exposed only through API), our work demonstrates that white-box access enables substantially  
1520 performance improvements, while remaining computationally efficient. Consequently, our approach  
1521 paves the way for integrating robust UQ mechanisms directly into existing LLM-as-a-service systems,  
1522 which is highly useful for real-world applications.

1523 Nevertheless, one possible direction for adapting our technique to a black-box setting is to employ  
1524 an auxiliary white-box proxy LLM from which attention signals and logits can be extracted. Such a  
1525 proxy model may be effective because it can detect ambiguous or underspecified queries, thereby  
1526 capturing uncertainty patterns that partially mirror those of the black-box target model.

1528  
1529  
1530  
1531  
1532  
1533  
1534  
1535  
1536  
1537  
1538  
1539  
1540  
1541  
1542  
1543  
1544  
1545  
1546  
1547  
1548  
1549  
1550  
1551  
1552  
1553  
1554  
1555  
1556  
1557  
1558  
1559  
1560  
1561  
1562  
1563  
1564  
1565